DEUTSCHE BUNDESBANK
EUROSYSTEM

Discussion Paper

Deutsche Bundesbank
No 20/2026

Quantification of margin of conservatism category C: Correlations and quantification levels

Jan Henrik Wosnitza

Deutsche Bundesbank, Wilhelm-Epstein-Straße 14, 60431 Frankfurt am Main,
Postfach 10 06 02, 60006 Frankfurt am Main

Tel +49 69 9566-0

Please address all orders in writing to: Deutsche Bundesbank, Press and Public Relations Division, at the above address or via email: www.bundesbank.de/contact

Internet http://www.bundesbank.de

DOI https://doi.org/10.71734/DP-2026-20
ISBN 978-3-98848-079-8
ISSN 2941-7503

Quantification of Margin of Conservatism Category C: Correlations and Quantification Levels*

Jan Henrik Wosnitza
Deutsche Bundesbank

Abstract

Financial institutions are required to incorporate a margin of conservatism for the general estimation error (MoC C) into their probability of default (PD) estimates. This paper presents three key contributions to the quantification of MoC C. First, the European banking regulation allows financial institutions to choose between overlapping and non-overlapping one-year default rates for calculating their calibration targets, i.e., their long run average default rates (LRADRs). When overlapping one-year default rates are used, it is crucial to account for temporal dependencies to accurately calculate MoC C. We provide a MoC C quantification for overlapping one-year default rates. Second, the European Central Bank has established MoC C quantification at grade level rather than at calibration segment level as the standard. However, many financial institutions calculate their LRADRs at calibration segment level rather than at grade level. Therefore, we approximate the confidence level for MoC C quantification at grade level to achieve the same sum of risk weighted exposure amounts as the MoC C at calibration segment level. Third, we corroborate that the common practice of using the maximum likelihood estimator of asset correlation on samples with varying PDs results in a downward bias. We compensate for this downward bias using a simulation approach.

Keywords: asset correlation, credit risk, downward bias, margin of conservatism, default rates with overlapping one-year performance windows, simulation experiment.

JEL classification: C15, G21, G28.

* Contact address: Jan Henrik Wosnitza, Deutsche Bundesbank, Regional Office in North Rhine-Westphalia, Directorate Financial Supervision, Berliner Allee 14, 40212 Düsseldorf, Germany. Phone: +49 211 874-0. E-mail: Jan.Henrik.Wosnitza@bundesbank.de.
The author thanks Stefan Häfner, Thomas Liebetrau, Christoph Meinerding, and Marvin Plümer – for providing valuable input to the second and third section of this paper.
Dedicated to my grandmother, Mathilde Blödorn, in appreciation of her lifelong inspiration.

1 Introduction

Lending activities are a major source of risk for financial institutions. Therefore, preventing the underestimation of credit risk is vital for them (Aussenegg et al. 2011). To pre-empt underestimation of credit risk, the European banking regulation structures the probability of default (PD) estimation into two parts. First, financial institutions must accurately estimate the PDs of their obligors, resulting in the best estimate PDs. Second, Article 179 (1) (f) of the Capital Requirements Regulation[1] (CRR) obliges financial institutions to "add to [their best] estimates a margin of conservatism" to arrive at conservative PD estimates. This margin of conservatism (MoC) is composed of three categories. While categories A and B address rather institution-specific data, methodological, and representative issues, the nature of category C is much more general.

This paper contributes threefold to the quantification of MoC C. First, Paragraph 80 of the EBA Guidelines on PD estimation, LGD Estimation and the Treatment of Defaulted Exposures[2] (EBA/GL/2017/16) allows financial institution to choose "between an approach based on overlapping and an approach based on non-overlapping one-year time windows" to calculate the calibration target level (i.e. the long run average default rate (LRADR)) for their PD estimates. The European Central Bank expects that financial institutions quantify the MoC C based on the distribution of the chosen LRADR (see Paragraph 210 (a) of the ECB Guide to Internal Models[3] (EGIM)). While an emerging body of literature deals with the MoC C quantification in the case of default rates with non-overlapping one-year performance windows (hereafter referred to as non-overlapping one-year default rates) (Casellina et al. 2023; Lawrenz 2008; Rösch 2004; Scherer et al. 2023; Wosnitza 2025), MoC C quantification in the case of overlapping one-year default rates represents a research gap. We fill this research gap by deriving an equation for MoC C in the case of overlapping one-year default rates, explicitly incorporating the serial dependencies in monthly default counts.

Paragraph 210 (a) of the EGIM has established MoC C quantification at grade level rather than at calibration segment level as the standard.[4] However, many financial institutions calculate their calibration target levels (i.e. their LRADRs) at calibration segment level rather than at grade level. Therefore, we approximate the confidence level for MoC C quantification at grade level that results in the same sum of risk weighted exposure amounts (RWEAs) as the MoC C at calibration segment level for a given confidence level as a second contribution. To this end, we also explore the aggregation of best estimate PDs and MoC C at calibration segment level to derive conservative PDs.

[1] European Parliament and Council 2013.
[2] European Banking Authority 2017.
[3] European Central Bank 2024.
[4] While the calibration segment level aggregates all obligors across different grades for joint calibration, the grade level considers only those obligors assigned to a particular grade.

Third, there is a broad consensus in both the banking sector and the financial literature that the assumption of independent defaults is generally inappropriate for credit risk modelling purposes (e.g. Huschens et al. (2005)). Wosnitza (2025) reveals that the intra-year dependency[5] of default events is also a key driver of MoC C. Although the question is still open (Wosnitza 2023b), we believe that the European banking regulation allows financial institutions to estimate these default dependencies themselves for the purpose of MoC C quantification[6] rather than relying on the regulatory asset correlations defined in Article 153 1 (iii) and Article 154 1 (ii) of the CRR. Financial institutions usually derive asset correlations from two kinds of data. If the required data are available, they use "the correlation between equity returns as a proxy for the correlation of asset returns" as suggested by RiskMetrics Group (1997). In many retail portfolios, however, the derivation of asset correlations from equity returns is either impossible or inadequate. In these cases, financial institutions fall back on time series of default rates to estimate asset correlations. For one thing, this makes the asset correlation estimates vulnerable to structural breaks such as the introduction of a new bankruptcy code (Duellmann et al. 2010). For another, previous literature revealed that correlation "estimates from default rates are typically downward biased" (e.g. Duellmann et al. (2010), Geidosch (2014)). More specifically, Wunderer (2019) studies the systematic error that financial institutions commit if the they incorrectly assume that the sample underlying the default rates is homogeneous with respect to PD. He finds that the downward bias is larger, the more spread out the PDs are within the estimation sample. Several financial institutions seek to counteract this downward bias by employing the upper endpoint of a certain confidence interval rather than the best estimate of the asset correlation. We corroborate the findings of Wunderer (2019) and reveal that the upper endpoints of standard confidence intervals are insufficient to compensate fully for the downward bias. Therefore, we compensate for this downward bias using a simulation approach.

The structure of the paper is as follows. Sections 2, 3, and 4 are devoted to the detailed exposition of the three contributions, respectively. Section 5 concludes with a summary of the key results.

---

[5] Please note that several terms are used to describe default dependency. This paper employs the terms "default correlation" and "asset correlation". While asset correlation reflects the dependency between the solvency variables of two individual obligors, default correlation captures the dependency between the default events of those same obligors (Huschens et al. (2005)). We can convert asset correlation into default correlation using the equation presented at the top of p. 333 in Bluhm et al. (2010) or Equation (19) of Huschens et al. (2005).

[6] Financial institutions also estimate asset correlations as part of the second pillar of the Basel Capital Accord.

2 MoC C quantification for overlapping one-year default rates

This section quantifies the MoC C in the context of overlapping one-year default rates, explicitly accounting for serial dependencies in monthly default counts. To achieve this, we first introduce two key assumptions and subsequently calculate the long run average default rate (LRADR). Building on this foundation, we derive the variance of the LRADR and then apply a Central Limit Theorem to demonstrate that the LRADR converges to a normal distribution, even when one-year default rates overlap. The mean and variance together fully characterize this normal distribution. For completeness, Appendix A shows that our methodology is consistent with the European Central Bank's expectation that "the shorter the time series are, the higher the MoC [C] of the grade should be".

Let the random variable D_t denote the number of defaults that occur in month t. The first assumption is that the random variables D_t with $t = 1,2,\dots,T-1,T$ are identically distributed. The deterministic variable N_t stands for the number of non-defaulted obligors at the beginning of period t. The difference between the number of non-defaulted obligors at the beginning of two consecutive periods $t-1$ and t is equal to the difference between the number of new obligors Δ_{t-1}, the number of defaulted obligors D_{t-1}, and the number of paid-off obligors δ_{t-1} in period $t-1$:

$$N_t - N_{t-1} = \Delta_{t-1} - D_{t-1} - \delta_{t-1} \tag{1}$$

The second assumption is that the number of non-defaulted obligors at the beginning of each month t is constant over time, i.e. $N_t = N_1$ for all $t \in \{2,\dots,T\}$. In other words, the number of new obligors Δ_t in period t compensates the sum of defaults D_t and paid-off obligors δ_t in period t, i.e. $\Delta_t = D_t + \delta_t$ for all t. Based on these two assumptions, we can express the one-year default rate of month t as follows:

$$DR_t = \frac{1}{N_1} \cdot \sum_{\tau=0}^{11} D_{t+\tau}. \tag{2}$$

To calculate the calibration target, i.e. the long run average default rate (LRADR), we average the overlapping one-year default rates in the next step. T stands for the length of the historical observation period in months and the detailed derivation can be found in Appendix B:

$$\frac{1}{T} \cdot \sum_{t=1}^{T} DR_t = \sum_{t=1}^{T+11} \frac{a_t}{\sqrt{T}} \cdot D_t, \tag{3}$$

where $a_t = \begin{cases} \frac{t}{\sqrt{T}\cdot N_1} \text{ for } 1 \le t \le 11 \\ \frac{12}{\sqrt{T}\cdot N_1} \text{ for } 12 \le t \le T \\ \frac{(T+11)-(t-1)}{\sqrt{T}\cdot N_1} \text{ for } T+1 \le t \le T+11 \end{cases}$. Please note that the MoC C quantification approach in this paper is based on a slightly different default rate definition than the definition given in Paragraph 73 (b) of EBA/GL2017/16. Paragraph 73 (b) stipulates

- "that the denominator [of the one-year default rate] consists of the number of non-defaulted obligors with any credit obligation observed at the beginning of the one-year observation period" and
- "that the numerator [of the one-year default rate] includes all those obligors considered in the denominator that had at least one default event during the one-year observation period."

In contrast, the default rate definition applied in Equation (3) does not only count the default events of those obligors with any credit obligation observed at the beginning of the one-year observation period. In fact, the numerator also counts default events of obligors that enter the portfolio after the beginning of the one-year observation period and default within this one-year period. We can think of the number of "extra defaults" as an additional random variable. Under the assumption that the number of "extra defaults" is not negatively correlated with the number of "regulatory defaults", Equation (4) will overestimate the true variance of the LRADR.

We now present an approximate expression for the variance of the LRADR in the case of overlapping one-year default rates, based on Equation (3). For a detailed derivation, see Appendix C:

$$\mathbb{V}\left[\frac{1}{T}\cdot\sum_{t=1}^{T} DR_t\right] \approx \frac{1}{T}\cdot\left(\frac{12}{N_1}\right)^2\cdot\left(\mathbb{V}[D_t] + 2\cdot\sum_{\Delta=1}^{T}\mathbb{Cov}[D_t, D_{t-\Delta}]\right). \tag{4}$$

This approximation is accurate when T is much greater than $\frac{143+3\cdot\Delta}{36}$.

Having established an approximate expression for the variance of the LRADR, our consideration now turns to its asymptotic distribution. For this purpose, we assume that the sequence $\{DR_t\}_{1\leq t\leq T}$ is stationary[7] and mixing[8], and satisfies the following conditions, together with an additional technical requirement:

- $\mathbb{E}[DR_t] < \infty$,
- $\mathbb{V}[DR_t] < \infty$, and
- $\lim_{T\to\infty}\left\{T\cdot\mathbb{V}\left[\frac{1}{T}\cdot\sum_{t=1}^{T} DR_t\right]\right\} \overset{\text{Eq. (4)}}{=} \left(\frac{12}{N_1}\right)^2\cdot\left(\mathbb{V}[D_t] + 2\cdot\sum_{\Delta=1}^{T}\mathbb{Cov}[D_t, D_{t-\Delta}]\right) = V < \infty.$

Under these assumptions, a Central Limit Theorem applies to the LRADR:

$$\frac{\sum_{t=1}^{T} DR_t - T\cdot\mathbb{E}[DR_t]}{\sqrt{T\cdot V}} \xrightarrow{d} Z,$$

where $\xrightarrow{d}$ indicates convergence in distribution and Z is a standard normal random variable.

[7] A sequence of random variables is stationary if the joint distribution of any set of adjacent terms is invariant under shifts in their position within the sequence.

[8] A sequence is mixing if the dependence between any two groups of terms diminishes as the groups become more widely separated, so that distant groups are nearly independent.

3 Harmonizing MoC C between calibration segment level and grade level

On the one hand, Paragraph 210 (a) of the EGIM establishes MoC C quantification at grade level as the standard, rather than at calibration segment level. On the other hand, many financial institutions calculate their calibration target levels (i.e. their LRADRs) at calibration segment level rather than at grade level. Therefore, the objective of this section is to approximate the confidence level for MoC C quantification at grade level that results in the same sum of risk weighted exposure amounts (RWEAs) as the MoC C at calibration segment level, associated with a specific confidence level. In summary, we need to multiply the MoCs C at grade level by the ratio of the variance of the default rate at calibration segment level divided by a weighted average of the variances of the default rates at grade level to achieve this equality. As the weights do not necessarily sum to one, we refer to this average as non-normalized weighted average.

We begin with the equation for the RWEAs for retail exposures as outlined in Article 154 of the CRR.[9] In this section, we calculate conservative PDs in two different ways. The first approach involves breaking down the MoC C at calibration segment level to the individual grades, specifically using $PD_k + \overbrace{\frac{PD_k}{LRADR}}^{=\beta_k} \cdot MoC$. Appendix E provides a detailed derivation of this approach. Alternatively, we apply a grade level-specific MoC C, which may have a different confidence level than the MoC C at calibration segment level, and incorporate it into the grade level PD using $PD_k + \alpha \cdot MoC_k$. In order to address both cases simultaneously, we input the synthesized yet more general conservative PDs $PD_k + \alpha \cdot \overbrace{\frac{PD_k}{LRADR}}^{=\beta_k} \cdot MoC_k$ into the equation for the RWEAs. Furthermore, we substitute $a_k = \sqrt{R(PD_k)} \cdot \Phi^{-1}(99.9\%)$, $b_k = \sqrt{1 - R(PD_k)}$, $\beta_k = \frac{PD_k}{LRADR}$, and $c_{i_k} = 12.5 \cdot 1.06 \cdot EAD_{i_k} \cdot LGD_{i_k}$ in order to simplify notation. The index k refers to rating class k and i_k stands for obligor i in rating class k:

[9] The mathematical derivation for non-retail exposures proceeds analogously. However, we expand the equation for risk weights using a Taylor series around $MoC_k = 0$. According to Paragraph 210 (a) of the EGIM, the ECB expects that a higher number of observations per grade should result in a lower MoC for that grade. Consequently, we consider this Taylor approximation to be most appropriate for retail portfolios.

$$RWEA(MoC_k) = \underbrace{12.5 \cdot 1.06 \cdot EAD_{i_k} \cdot LGD_{i_k}}_{=c_{i_k}} \cdot \left\{ \Phi \left[\frac{\Phi^{-1}\left(PD_k + \alpha \cdot \overbrace{\frac{PD_k}{LRADR}}^{=\beta_k} \cdot MoC_k \right) + \overbrace{\sqrt{R(PD_k)} \cdot \Phi^{-1}(99.9\%)}^{=a_k}}{\underbrace{\sqrt{1 - R(PD_k)}}_{=b_k}} \right] - \left(PD_k + \alpha \cdot \overbrace{\frac{PD_k}{LRADR}}^{=\beta_k} \cdot MoC_k \right) \right\} \tag{5}$$

Our objective is to determine the scaling factor α, which ensures that the MoC C at grade level yields a sum of RWEAs closely matching the sum produced by the MoC C at calibration segment level, i.e.

$$\sum_k \left\{ \Phi \left[\frac{\Phi^{-1}(PD_k + \beta_k \cdot MoC) + a_k}{b_k} \right] - (PD_k + \beta_k \cdot MoC) \right\} \cdot C_k \stackrel{!}{=} \sum_k \left\{ \Phi \left[\frac{\Phi^{-1}(PD_k + \alpha \cdot MoC_k) + a_k}{b_k} \right] - (PD_k + \alpha \cdot MoC_k) \right\} \cdot C_k, \tag{6}$$

where we substitute the sum $\sum_{i_k} c_{i_k}$ with the symbol C_k. While we apply the aggregation methodology developed in Appendix E to break down the MoC C at calibration segment level to the individual grades on the left-hand side, we simply add the MoC C at grade level to the best estimate PD at grade level on the right-hand side. In the next step, we linearize this optimization problem. More specifically, we expand the function $RWEA(MoC_k)$ in a Taylor Series around $MoC_k = 0$ up to the first order. To this end, we differentiate $RWEA(MoC_k)$ with respect to MoC_k using the chain rule; a comprehensive derivation is provided in Appendix F:

$$\frac{\partial}{\partial MoC_k} RWEA(MoC_k) = \frac{\alpha \cdot \beta_k}{b_k} \cdot C_k \cdot \left\{ \exp\left\{ -\frac{1}{2} \cdot \frac{1 - b_k^2}{b_k^2} \cdot \left(x_k + \frac{a_k}{1 - b_k^2} \right)^2 + \frac{a_k^2}{2 \cdot (1 - b_k^2)} \right\} - b_k \right\}, \tag{7}$$

In the following, we resubstitute $a_k = \sqrt{R(PD_k)} \cdot \Phi^{-1}(99.9\%)$, $b_k = \sqrt{1 - R(PD_k)}$, $\beta_k = \frac{PD_k}{LRADR}$ and $x_k = \Phi^{-1}\left(PD_k + \alpha \cdot \overbrace{\frac{PD_k}{LRADR}}^{=\beta_k} \cdot MoC_k \right)$. The detailed steps of this substitution are provided in Appendix G; the resulting expression for $Moc_k = 0$ is:

$$\frac{\partial}{\partial MoC_k} RWEA(MoC_k)\Big|_{MoC_k=0} = \frac{\alpha \cdot \frac{PD_k}{LRADR}}{\sqrt{1-R(PD_k)}} \cdot C_k \cdot \left[\exp\left\{-\frac{1}{2} \cdot \frac{R(PD_k)}{1-R(PD_k)} \cdot \left(\Phi^{-1}(PD_k) + \frac{\Phi^{-1}(99.9\%)}{\sqrt{R(PD_k)}}\right)^2 + \frac{\Phi^{-1}(99.9\%)^2}{2}\right\} - \sqrt{1-R(PD_k)}\right]. \tag{8}$$

We proceed by linearizing $RWEA(MoC)$ on the left-hand side and $RWEA(MoC_k)$ on the right-hand side of Equation (6) as follows. All details of this linearization can be found in Appendix H:

$$\begin{aligned} \Leftrightarrow MoC \cdot \sum_k \overbrace{\frac{\frac{PD_k}{LRADR}}{\sqrt{1-R(PD_k)}} \cdot C_k \cdot \left\{\exp\left\{-\frac{1}{2} \cdot \frac{R(PD_k)}{1-R(PD_k)} \cdot \left(\Phi^{-1}(PD_k) + \frac{\Phi^{-1}(99.9\%)}{\sqrt{R(PD_k)}}\right)^2 + \frac{\Phi^{-1}(99.9\%)^2}{2}\right\} - \sqrt{1-R(PD_k)}\right\}}^{=\frac{PD_k}{LRADR} \cdot w_k} \\ \approx \alpha \cdot \sum_k \underbrace{\frac{1}{\sqrt{1-R(PD_k)}} \cdot C_k \cdot \left\{\exp\left\{-\frac{1}{2} \cdot \frac{R(PD_k)}{1-R(PD_k)} \cdot \left(\Phi^{-1}(PD_k) + \frac{\Phi^{-1}(99.9\%)}{\sqrt{R(PD_k)}}\right)^2 + \frac{\Phi^{-1}(99.9\%)^2}{2}\right\} - \sqrt{1-R(PD_k)}\right\}}_{=w_k} \cdot MoC_k \end{aligned} \tag{9}$$

Based on this approximation, we subsequently determine the scaling factor α as follows:

$$\alpha \approx \frac{\frac{MoC}{LRADR}}{\sum_k \frac{w_k}{\sum_{k'} PD_{k'} \cdot w_{k'}} \cdot MoC_k}. \tag{10}$$

Assuming a sufficiently large number of obligors, a standard MoC C quantification approach involves multiplying the standard deviation of the one-year default rate by a quantile factor and then dividing this product by the square root of the length of the historical observation period. Following this standard MoC C quantification approach, the quantile factors in the numerator and denominator at the end of Equation (H.1) cancel each other out, resulting in the following expression for α:

$$\Rightarrow \alpha \approx \frac{\frac{\sqrt{\mathbb{Var}(DR)}}{\sqrt{T_{CSL}} \cdot LRADR}}{\sum_k \frac{w_k}{\sum_{k'} PD_{k'} \cdot w_{k'}} \cdot \frac{\sqrt{\mathbb{Var}(DR_k)}}{\sqrt{T_{GL_k}}}} \tag{11}$$

where

- $\mathbb{Var}(DR)$ denotes the variance of the default rate of the entire calibration segment,
- $\mathbb{Var}(DR_k)$ stands for the variance of the default rate of grade k,
- T_{CSL} is the number of observations used for the estimation of the variance of the default rate at calibration segment level, i.e. $\mathbb{Var}(DR)$, and
- T_{GL_k} labels the number of observations used for the estimation of the variance of the default rate at grade level, i.e. $\mathbb{Var}(DR_k)$.

For example, financial institutions can apply Equation (23) of Rösch (2004) in order to estimate $\mathbb{Var}(DR)$ and Equation (7) of Wosnitza (2025) in order to estimate $\mathbb{Var}(DR_k)$. The product of α and the original quantile factor yields the new quantile factor. This new quantile factor ensures that the sum of RWEAs calculated using MoC C at grade level is approximately equal to the sum using MoC C at calibration segment level. If the numbers of observations used for the estimation of the variances are equal, i.e. $T_{GL_k} = T_{CSL}$, then Equation (11) simplifies as follows:

$$\Rightarrow \alpha \approx \frac{\frac{\sqrt{\mathbb{Var}(DR)}}{LRADR}}{\sum_k \frac{w_k}{\sum_{k'} PD_{k'} \cdot w_{k'}} \cdot \sqrt{\mathbb{Var}(DR_k)}} \tag{12}$$

In summary, we need to multiply the MoCs C at grade level by the ratio of the variance of the default rate at calibration segment level divided by a non-normalized weighted average of the variances of the default rates at grade level to achieve this equality. However, the weights do not necessarily sum to one. If this approximation of alpha is too crude, it can serve at least as an initial value for solving the exact Equation (6) using numerical methods.

4 Compensating the downward bias inherent in maximum likelihood estimates of asset correlations

Wunderer (2019) explores the systematic error arising from the incorrect assumption that the estimation sample for asset correlation is homogeneous with respect to PD. The author demonstrates that financial institutions often underestimate asset correlation when estimating this parameter from samples with heterogenous PDs. Furthermore, he reveals that the extent of this downward bias increases as the variability of PDs within the estimation sample rises. The objective of this section is to compensate for the downward bias inherent in maximum likelihood estimates of asset correlations derived from default rates. To achieve this, we first introduce the maximum likelihood estimator proposed by Düllmann and Trapp (2004) and examine the factors contributing to its downward bias in Subsection 4.1. In Subsection 4.2, we outline a widely used approach for calculating confidence intervals for the maximum likelihood estimator of asset correlation. Subsequently, in Subsection 4.3, we utilize the framework established by Wosnitza (2023a) to simulate time series of default rates for portfolios comprising a finite number of obligors with varying credit quality. To enhance the generality of our results, we generate time series of default rates for several combinations of asset correlation, discriminatory power, and unconditional PD, leading to two key findings. First, our results indicate that discriminatory power significantly contributes to the downward bias, consistent with the findings of Wunderer (2019). Second, we establish that conventional confidence bands, such as those at the 95% or 99% confidence levels, are inadequate for addressing this downward bias. Instead, we propose adjustment factors that fully compensate for the downward bias. To this end, we estimate the asset correlation from the synthetic time series of default rates for each combination of asset correlation, discriminatory power, and unconditional PD. Subsequently, we calculate the ratio of the true specified asset correlation divided by the estimated asset correlation.

4.1. Maximum likelihood estimator of asset correlation and reasons behind its downward bias

Düllmann and Trapp (2004) express the asset correlation as a function of the variance of transformed non-overlapping one-year default rates (DRs):

$$\rho = \frac{\mathbb{V}[\Phi^{-1}(DR_t)]}{1 + \mathbb{V}[\Phi^{-1}(DR_t)]} \tag{13}$$

where

- ρ denotes the asset correlation between any two distinct obligors in the respective portfolio and
- Φ^{-1} stands for the inverse of the standard normal cumulative distribution function.

Financial institutions often employ this maximum likelihood estimator to derive asset correlations from time series of default rates. To this end, they estimate the variance of the transformed default rates using the sample variance and substitute this sample variance for $\mathbb{V}[\Phi^{-1}(DR_t)]$ into Equation (13). In order to demonstrate that the asset correlation is a strictly monotonically increasing function of $\mathbb{V}[\Phi^{-1}(DR_t)]$, we first substitute $\mathbb{V}[\Phi^{-1}(DR_t)]$ with x and then we differentiate the right-hand side of Equation (13) with respect to x:

$$\frac{\partial}{\partial x}\rho = \frac{\partial}{\partial x}\frac{x}{1+x} = \frac{(1+x)-x}{(1+x)^2} = \frac{1}{(1+x)^2} > 0. \tag{14}$$

Although maximum likelihood estimators are asymptotically unbiased, previous literature revealed that asset correlation "estimates from default rates are typically downward biased" (e.g. Duellmann et al. (2010), Geidosch (2014)). The first reason for this downward bias is that time series of DRs must be sufficiently long to fully exploit the advantages of maximum likelihood estimators. In real-world applications, the number of years T in the historical observation period hardly exceeds the value of 30. Indeed, Article 180 (1) (h) and (2) (e) of the CRR stipulate that the length of the historical observation period underlying the estimation of PDs (resp. of loss characteristics) shall be at least five years (for at least one source). Moreover, Paragraph 82 of the EBA/GL/2017/16 requires that "additional observations to the most recent 5 years, at the time of model calibration, should be considered relevant when these observations are required in order for the historical observation period to reflect the likely range of variability of default rates of that type of exposures […]." With such a short historical observation period, the asymptotic properties of the MLEs do not yet fully develop.

Furthermore, the derivation by Düllmann and Trapp (2004) is based on a stylized credit portfolio, specifically one that consists of an infinite number of obligors with equal PDs. However, the rating grades at the extremes of the rating distribution typically contain too few obligors to accurately estimate default correlation for each rating grade. To better align with the assumption of an infinite number of obligors, banks often aggregate obligors from different rating grades. However, this practice contravenes the assumption of a homogeneous estimation sample with regard to PD. Subsection 4.3 confirms that the violation of the assumption of equal PDs constitutes the second reason for the downward bias observed in the maximum likelihood estimator of asset correlation.

4.2. Confidence interval for maximum likelihood estimator of asset correlation

In this subsection, we first present the methodology proposed by Höse and Huschens (2010) to construct confidence intervals for the true asset correlation, based on a specified confidence level. Second, we utilize the upper endpoint of this confidence interval as a conservative estimate of the true unknown asset correlation. As previously mentioned in Subsection 4.1, the standard procedure for estimating asset correlations from Equation (13) involves substituting the variance of the transformed default rates $\mathbb{V}[\Phi^{-1}(DR_t)]$ with its sample variance s^2. According to Equation (14), the asset correlation is a strictly monotonically increasing function of $\mathbb{V}[\Phi^{-1}(DR_t)]$. Therefore, we can derive a conservative estimate of the asset correlation by substituting the sample variance with its upper bound.

It is a well-established fact that the sample variance derived from T independent normally distributed observations, when scaled by $\frac{T-1}{\sigma^2}$, follows a chi-squared distribution with $T-1$ degrees of freedom. By substituting the variance of the transformed default rates in Equation (13) with the upper endpoint of the two-sided $(1-\alpha)$-confidence interval for the sample variance, given by $\frac{(T-1)\cdot s^2}{\chi^2_{T-1,\frac{\alpha}{2}}}$, we obtain the following conservative estimate for the asset correlation:

$$\hat{\rho}_{\text{conservative}} = \frac{\frac{(T-1)\cdot s^2}{\chi^2_{T-1,\frac{\alpha}{2}}}}{1+\frac{(T-1)\cdot s^2}{\chi^2_{T-1,\frac{\alpha}{2}}}} \cdot \frac{\frac{\chi^2_{T-1,\frac{\alpha}{2}}}{1}}{\frac{\chi^2_{T-1,\frac{\alpha}{2}}}{1}} = \frac{(T-1)\cdot s^2}{(T-1)\cdot s^2+\chi^2_{T-1,\frac{\alpha}{2}}}. \tag{15}$$

4.3. Measuring the downward bias of asset correlation from synthetic time series of default rates

As we cannot directly observe realizations of asset correlations, comparing realized asset correlations with their estimates is not feasible. Consequently, in this subsection, we design and conduct a simulation experiment using synthetic time series of default rates, with three primary objectives. First, we seek to validate the findings of Wunderer (2019), which suggest that violating the assumption of equal PDs leads to a downward bias in the estimation of asset correlation. Second, the simulation experiment demonstrates that conventional confidence bands, such as those at the 95% or 99% confidence level, are inadequate for mitigating this bias. Finally, we introduce adjustment factors that fully compensate for this downward bias as a third innovation.

The following outlines our simulation environment for estimating asset correlations from synthetic time series of default rates spanning T consecutive one-year periods in four distinct steps. Given that a historical observation period of 20 years includes the late-2000s financial crisis, we set $T = 20$ for this section. In the first step, we define the values of the three key parameters as follows:

- The asset correlation varies from 0% to 30% in increments of 2.5%, thereby encompassing and slightly extending the range of values set out in Article 153 and Article 154 of the CRR.
- The unconditional PD ranges from 0.5% to 8%, doubling with each increment. The exclusion of unconditional PDs below 0.5% is consistent with EBA/GL/2017/16 (p. 18), which states that portfolios with very low default rates may require alternative approaches for MoC C quantification to avoid disproportionate conservatism.
- The preliminary (theoretical) discriminatory power, measured by the AUROC, ranges from 0.5 to 0.975 in increments of 0.025, reflecting the broad spectrum of discriminatory power observed in practice. This parameter represents the AUROC before accounting for asset correlation. Since both randomness and asset correlation affect discriminatory power, we analyzed the estimated asset correlation as a function of the final (empirical) AUROC and the true asset correlation for different unconditional PDs. The final (empirical) AUROC was defined in three ways:
    - o as the average of the AUROC values calculated separately for each year within the 20-year historical observation period,

- as the median of the AUROC values calculated separately for each year within the 20-year period, and
- as the AUROC calculated from the pooled credit scores and default statuses over the entire 20-year period.

All of these figures are qualitatively very similar to those based on the preliminary (theoretical) discriminatory power. For completeness, we have shifted the figures to the Appendix J for the interested reader.

After defining these three-tuples, we adhere to the simulation framework established by Wosnitza (2023a) to generate synthetic time series of default rates for each tuple in the second step. Specifically, we construct two normal distributions. The first represents the distribution of credit scores for defaults, while the second corresponds to the distribution of credit scores for non-defaults. The variance of both normal distributions is set to one, and the negative mean of the credit score distribution for defaults is equal to the mean of the credit score distribution for non-defaults. These distributional assumptions indicate that obligors with low credit quality tend to have lower credit scores than those with high credit quality. Following Equation (3.14) from Tasche (2010), we select the mean of the credit score distribution for non-defaults to align with the specified AUROC. The AUROC measures the ability of a PD model to discriminate between future defaults and non-defaults; a value of one-half indicates no discriminatory power, while a value of one signifies perfect discrimination.[10] From these two normal distributions, we randomly sample credit scores of defaults and non-defaults, respectively.

We convert these credit scores into individual PDs for the obligors using a logistic regression model. Within the context of the two normal distributions, the logistic regression model provides the PDs of the obligors as Wosnitza (2023a) explains. We then use these obligor-specific PDs to simulate the default rate of the portfolio within the framework of the credit portfolio model of Vasicek (1987). The simulation begins with the generation of asset values which involves drawing an independent standard normally distributed systematic factor, Y_t, as well as independent standard normally distributed idiosyncratic factors, $\varepsilon_{t,k}$, for all obligors $k \in \{1, \dots, n\}$. We set $n = 10{,}000$ for the purpose of this section. These idiosyncratic factors are also independent of the systematic factor. The asset value $A_{k,t}$ of obligor k is calculated as a weighted sum of the systematic factor and the idiosyncratic factor, with the asset correlation determining the weights. More specifically, we perform 100 independent random draws for the systematic factor and the idiosyncratic factors, rather than relying on a single draw. This approach reduces the dependency of the results on any random seed, thereby enhancing robustness and reliability.

If the asset value of an obligor is below his individual default threshold $\Phi^{-1}(PD_k)$ at the end of the designated risk horizon (typically one year), we classify this obligor as having defaulted. Situations in which the asset value breaches the default threshold prior to the end of the risk horizon, but the obligor subsequently "cures" before the risk horizon concludes, are not considered defaults. The total number of default events constitutes the numerator, $d(t)$, for the portfolio's default rate. If $n(t)$ represents the number of obligors at the beginning of period t,

[10] Furthermore, lower discriminatory power results in greater variability of the default rates.

then the default rate is calculated as $\frac{d(t)}{n(t)}$. We repeat these steps to generate time series of default rates of specified length.

In the third step, we employ the maximum likelihood estimator from Equation (8) of Düllmann and Trapp (2004) to estimate the asset correlation based on these synthetic time series of default rates. A key advantage of this simulation design is that we know the true value of the asset correlation from the outset. This allows us to accurately measure the estimation error by comparing the known true asset correlations with their estimates.

The following figures illustrate the difference between the predefined asset correlation and the mean estimated asset correlation across 100 random draws of the systematic factor and the idiosyncratic factors, as a function of discriminatory power and predefined asset correlation for several unconditional PDs.[11] These figures demonstrate that asset correlations derived from time series of default rates (represented by the dark grey surface) tend to underestimate the predefined asset correlations (depicted by the light grey surface). Notably, the downward bias intensifies with higher AUROC values and greater asset correlations. This observation consistently holds across all unconditional PDs investigated. Consequently, our results suggest that financial institutions should calibrate their corrections on a case-by-case basis to effectively address this underestimation.

Financial institutions seek to mitigate this downward bias by utilizing the upper endpoint of a specific confidence interval rather than relying on the best estimate of the asset correlation. Specifically, they typically employ Equation (15) to calculate this upper endpoint. We examine the level of confidence required to offset the downward bias. Our findings indicate that conventional confidence bands, such as those at the 95% or 99% confidence level, do not fully mitigate this downward bias. Therefore, we propose using the ratio of the predefined values of the asset correlation (i.e. the values represented by the light grey surface) to the estimated asset correlation values (i.e. the values represented by the dark grey surface) as correction factors. These adjustment factors are tailored to the following variables: discriminatory power, asset correlation, unconditional PD, number of obligors, and length of the historical observation period.

[11] Please note that Appendix I presents the difference between the predefined asset correlation and the median estimated asset correlation across the 100 random draws of the systematic factor and the idiosyncratic factors for the same unconditional PDs.

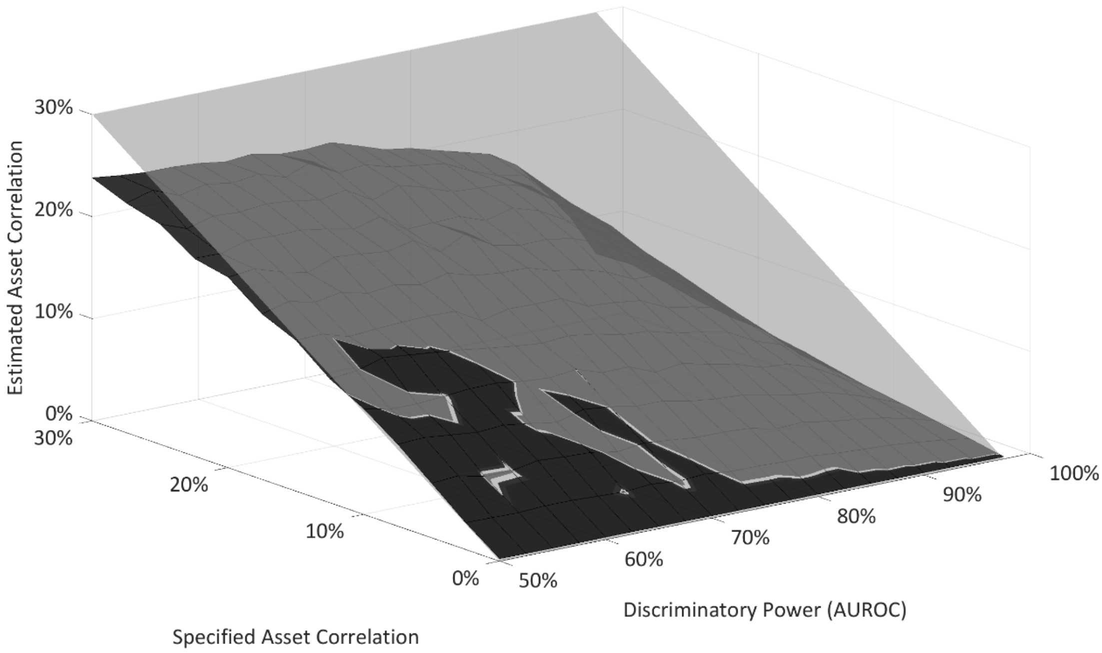

Figure 1: Comparison of theoretical (light grey surface) and average estimated (dark grey surface) asset correlation across 100 random draws of the systematic and idiosyncratic factors, shown as a function of the preliminary (theoretical) discriminatory power (measured by the AUROC) and predefined asset correlation. The unconditional PD is set to 0.5%. The figure illustrates that asset correlations estimated from time series of default rates (dark grey surface) tend to underestimate the predefined asset correlation (light grey surface). The extent of underestimation of the asset correlation varies with the preliminary (theoretical) discriminatory power (AUROC) and the true predefined asset correlation.

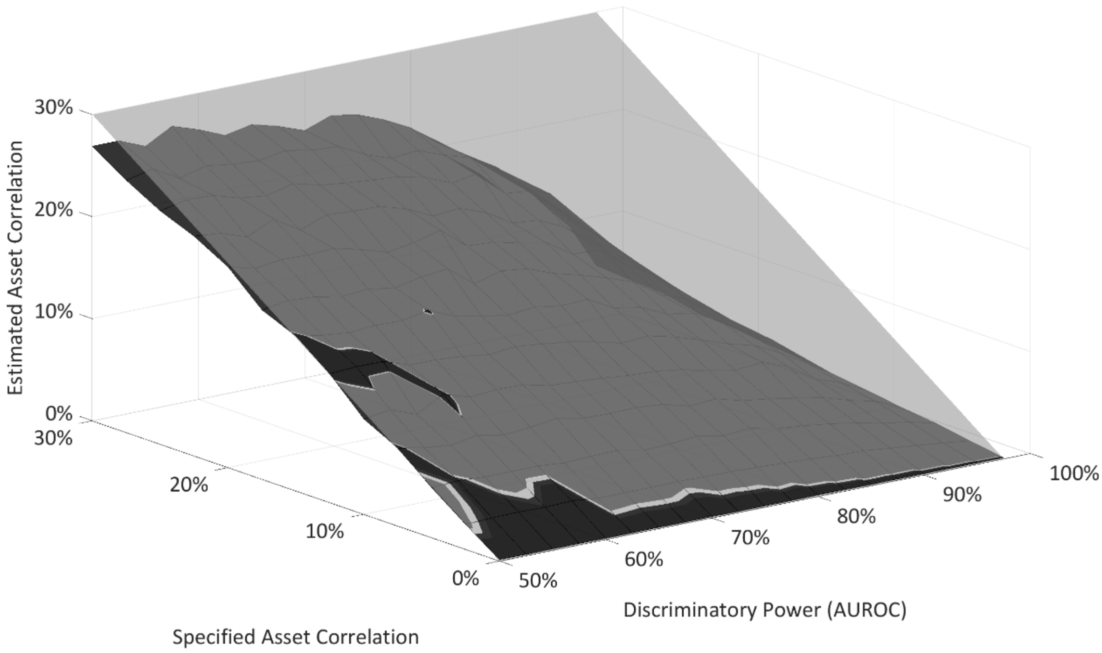

Figure 2: Comparison of theoretical (light grey surface) and average estimated (dark grey surface) asset correlation across 100 random draws of the systematic and idiosyncratic factors, shown as a function of the preliminary (theoretical) discriminatory power (measured by the AUROC) and predefined asset correlation. The unconditional PD is set to 1.0%. The figure illustrates that asset correlations estimated from time series of default rates (dark grey surface) tend to underestimate the predefined asset correlation (light grey surface). The extent of underestimation of the asset correlation varies with the preliminary (theoretical) discriminatory power (AUROC) and the true predefined asset correlation.

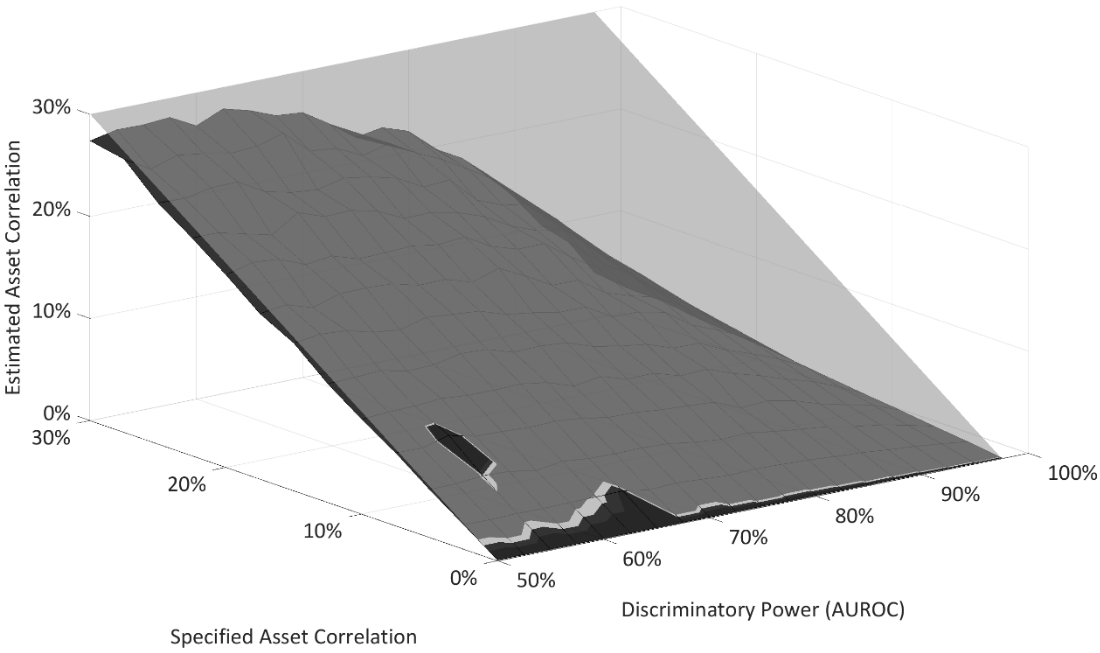

Figure 3: Comparison of theoretical (light grey surface) and average estimated (dark grey surface) asset correlation across 100 random draws of the systematic and idiosyncratic factors, shown as a function of the preliminary (theoretical) discriminatory power (measured by the AUROC) and predefined asset correlation. The unconditional PD is set to 2.0%. The figure illustrates that asset correlations estimated from time series of default rates (dark grey surface) tend to underestimate the predefined asset correlation (light grey surface). The extent of underestimation of the asset correlation varies with the preliminary (theoretical) discriminatory power (AUROC) and the true predefined asset correlation.

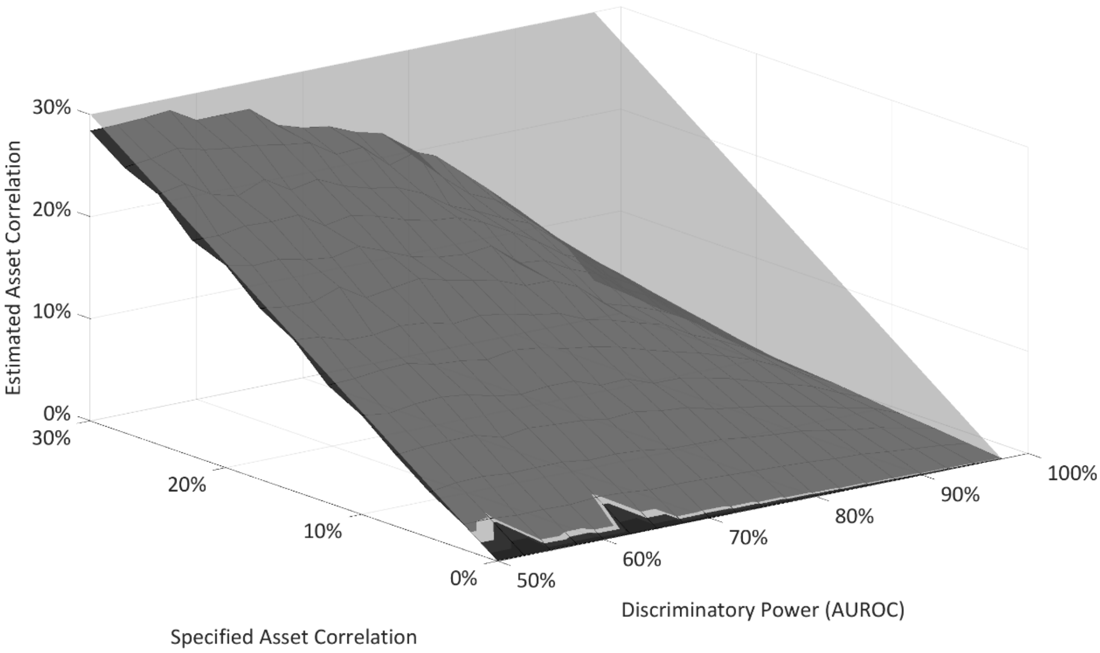

Figure 4: Comparison of theoretical (light grey surface) and average estimated (dark grey surface) asset correlation across 100 random draws of the systematic and idiosyncratic factors, shown as a function of the preliminary (theoretical) discriminatory power (measured by the AUROC) and predefined asset correlation. The unconditional PD is set to 4.0%. The figure illustrates that asset correlations estimated from time series of default rates (dark grey surface) tend to underestimate the predefined asset correlation (light grey surface). The extent of underestimation of the asset correlation varies with the preliminary (theoretical) discriminatory power (AUROC) and the true predefined asset correlation.

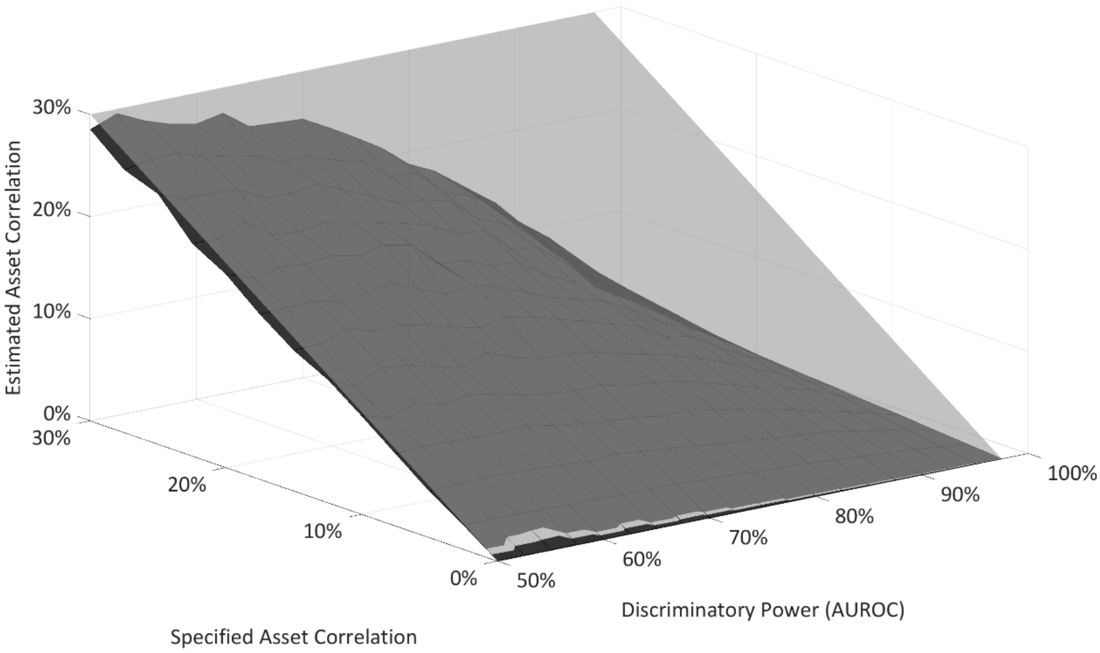

Figure 5: Comparison of theoretical (light grey surface) and average estimated (dark grey surface) asset correlation across 100 random draws of the systematic and idiosyncratic factors, shown as a function of the preliminary (theoretical) discriminatory power (measured by the AUROC) and predefined asset correlation. The unconditional PD is set to 8.0%. The figure illustrates that asset correlations estimated from time series of default rates (dark grey surface) tend to underestimate the predefined asset correlation (light grey surface). The extent of underestimation of the asset correlation varies with the preliminary (theoretical) discriminatory power (AUROC) and the true predefined asset correlation.

5 Conclusion

The European banking regulation allows financial institutions to calculate the LRADR using either overlapping or non-overlapping one-year default rates. While existing literature addresses MoC C quantification for non-overlapping one-year default rates, a research gap persists regarding overlapping one-year default rates. This paper fills this gap by deriving a formula for the variance of the LRADR that explicitly incorporates dependencies between monthly default counts. This formula provides model developers with a means to quantify MoC C in the case of overlapping one-year default rates. In addition, banking supervisors can use this approach to challenge and assess MoC C quantification levels in this context, thereby supporting a more rigorous supervisory review.

An important limitation of our analysis is the simplifying assumption that the number of non-defaulted obligors remains constant over time. In practice, the obligor population is itself a random variable, influenced by new lending, repayments, and defaults, which may fluctuate with changing economic conditions. Relaxing this assumption and explicitly modeling the dynamics of the obligor pool could provide more realistic and nuanced insights. We consider this a promising direction for future research.

Paragraph 210 (a) of the EGIM has established MoC C quantification at grade level rather than at calibration segment level as the standard. However, many financial institutions calculate their calibration target levels (i.e., LRADRs) at calibration segment level rather than at grade level. Therefore, our second main contribution is the approximation of the confidence level for MoC C quantification at grade level that results in the same sum of RWEAs as the MoC C at calibration segment level. In doing so, we take advantage of the fact that the current regulatory framework does not prescribe any specific confidence level for MoC C quantification. In summary, we need to multiply the MoCs C at grade level by the ratio of the variance of the default rate at calibration segment level divided by a non-normalized weighted average of the variances of the default rates at grade level to achieve this equality. Following this approach, there is no material difference in the overall own funds requirements, regardless of whether financial institutions quantify MoC C at grade level or at calibration segment level. As basis to arrive at this second main contribution, we develop a methodology to aggregate best estimate PDs and MoC C at calibration segment level into conservative PDs within the framework of logistic regression.

In the context of perfect point-in-time risk differentiation, the ratings of the obligors reflect their current credit quality. The obligors change their rating grades according to their credit quality, and the default rates of the rating grades remain constant over time. Consequently, both the variance of the one-year default rates and the MoC C at the grade level are low. In contrast, through-the-cycle ratings reflect the credit quality of obligors throughout the entirety of the economic cycle. Consequently, obligors typically remain within their assigned rating grades throughout the entire economic cycle, while the default rates associated with these rating grades fluctuate over time. This implies that both the variance of the one-year default rates and the MoC C at the grade level are high. Our proposed approach allows for the quantification of MoC C at grade level without the rating philosophy influencing the level of MoC C at calibration segment level.

According to Equation (7) of Wosnitza (2025), intra-year dependencies of default events are a main driver of MoC C. However, Duellmann et al. (2010) unveil that correlation estimates from default rates are downward biased. More precisely, Wunderer (2019) reveals a bias introduced by financial institutions when they mistakenly assume that the sample underlying the default rates is homogeneous in terms of PD. This downward bias can directly lead to a downward bias in MoC C. In order to compensate for this downward bias, we employ the simulation framework established by Tasche (2010) and refined by Wosnitza (2023a). Under these clinical conditions, we simulate time series of synthetic default rates and estimate the asset correlation as a function of the true asset correlation and discriminatory power (measured by the AUROC) for different values of the unconditional PD. Our key findings are as follows. In line with Wunderer (2019), we first observe that the downward bias intensifies as the discriminatory power of the underlying PDs increases, and it also increases with higher asset correlations. Therefore, we confirm that the prevalent practice among financial institutions of grouping obligors with varying PDs to expand the estimation sample (rather than estimating asset correlations by rating grades) exacerbates the downward bias. Second, our results indicate that common confidence bands, such as those at the 95% or 99% confidence level, do not fully account for the downward bias inherent in the maximum likelihood estimator of asset correlations. Therefore, internal validation functions and external banking supervisors should require financial institutions to carefully justify their levels of confidence to counteract the downward bias of asset correlations estimated from default rates. Third, we derive adjustment factors that fully compensate for the downward bias.

Financial institutions use credit portfolio models in the second pillar of the Basel Capital Accord to aggregate their credit risk. One key parameter that feeds into these credit portfolio models is the asset correlation, which captures intra-year default dependencies among obligors. According to Duellmann et al. (2010), “asset correlations are a key driver of credit risk”. Furthermore, Pfeuffer et al. (2020) state that the asset correlation “has a tremendous impact on the tail of the resulting loss distribution”. Because of its “tremendous impact”, downward biased estimates of the asset correlation can lead to an underestimation of credit risk in the second pillar of the Basel Capital Accord and, consequently, jeopardize the bank‘s solvency. Therefore, our results are also pertinent to economic capital quantification. Moreover, Paragraph 85 of the ECB Guide to the Internal Capital Adequacy Assessment Process (European Central Bank 2018) requires financial institution “to take a prudent approach whenever assuming risk diversification effects”. By performing 100 independent random draws for both systematic and idiosyncratic factors, our approach enables financial institutions to select a specific quantile (i.e., a conservative estimate) rather than relying on the average or median (i.e., a best estimate) for Pillar Two purposes.

List of references

Aussenegg, Wolfgang; Resch, Florian; Winkler, Gerhard (2011): Pitfalls and remedies in testing the calibration quality of rating systems. In *Journal of Banking & Finance* 38 (3), pp. 698–708. Available online at https://doi.org/10.1016/j.jbankfin.2010.11.016.

Bluhm, Christian; Overbeck, Ludger; Wagner, Christoph (2010): Introduction to credit risk modeling. Boca Raton, Florida, London [England], New York: CRC Press, Taylor & Francis Group (Chapman & Hall/CRC Financial Mathematics Series).

Casellina, Simone; Landini, Simone; Uberti, Mariacristina (2023): Credit risk measures and the estimation error in the ASRF model under the Basel II IRB approach. In *Communications in Nonlinear Science and Numerical Simulation* 118, Article 106977. DOI: 10.1016/j.cnsns.2022.106977.

Duellmann, Klaus; Küll, Jonathan; Kunisch, Michael (2010): Estimating asset correlations from stock prices or default rates—Which method is superior? In *Journal of Economic Dynamics and Control* 34 (11), pp. 2341–2357. DOI: 10.1016/j.jedc.2010.06.003.

Düllmann, Klaus; Trapp, Monika (2004): Systematic Risk in Recovery Rates - An Empirical Analysis of Us Corporate Credit Exposures. In *Bundesbank Discussion Paper*, Article 02. Available online at https://www.bundesbank.de/en/publications/research/discussion-papers/systematic-risk-in-recovery-rates-an-empirical-analysis-of-us-corporate-credit-exposures-704154.

European Banking Authority (2017): Guidelines on PD estimation, LGD estimation and treatment of defaulted assets. EBA/GL/2017/16. Source: https://www.eba.europa.eu/regulation-and-policy/model-validation/guidelines-on-pd-lgd-estimation-and-treatment-of-defaulted-assets#pane-new-3cd4feaf-807f-4122-9d50-97dc4859d840.

European Central Bank (2018): ECB Guide to the internal capital adequacy assessment process (ICAAP). EGICAAP. Source: https://www.bankingsupervision.europa.eu/ecb/pub/pdf/ssm.icaap_guide_201811.en.pdf.

European Central Bank (2024): ECB guide to internal models. EGIM. Source: https://www.bankingsupervision.europa.eu/ecb/pub/pdf/ssm.supervisory_guides202402_internalmodels.en.pdf.

European Parliament and Council (2013): Corrigendum to Regulation (EU) No 575/2013 of the European Parliament and of the Council of 26 June 2013 on prudential requirements for credit institutions and investment firms and amending Regulation (EU) No 648/2012. CRR. Source: http://data.europa.eu/eli/reg/2013/575/corrigendum/2013-11-30/oj.

Geidosch, Marco (2014): Asset correlation in residential mortgage-backed security reference portfolios. In *The Journal of Credit Risk* 10 (2), pp. 71–95. DOI: 10.21314/JCR.2014.175.

Höse, Steffi; Huschens, Stefan (Eds.) (2010): Confidence lntervals for Asset Correlations in the Asymptotic Single Risk Factor Model. Annual International Conference of the German Operations Research Society. Munich, Germany, September 1-3. Berlin, Heidelberg: Springer. Available online at https://doi.org/10.1007/978-3-642-20009-0_18.

Huschens, Stefan; Vogl, Konstantin; Wania, Robert (2005): Estimation of Default Probabilities and Default Correlations. In Michael Frenkel, Markus Rudolf, Ulrich Hommel (Eds.): Risk management, pp. 239–258. Available online at https://doi.org/10.1007/3-540-26993-2_12.

Lawrenz, Jochen (2008): Assessing the Estimation Uncertainty of Default Probabilities. In *Kredit und Kapital* 41 (2), pp. 217–238. DOI: 10.3790/kuk.41.2.217.

Pfeuffer, Marius; Nagl, Maximilian; Fischer, Matthias; Rösch, Daniel (2020): Parameter estimation, bias correction and uncertainty quantification in the Vasicek credit portfolio model. In *Journal of Risk* 22 (4), pp. 1–30. DOI: 10.21314/JOR.2020.429.

RiskMetrics Group (1997): Credit Metrics. Technical Document. J.P. Morgan & Co. Available online at https://www.msci.com/documents/10199/93396227-d449-4229-9143-24a94dab122f.

Rösch, Daniel (2004): Regulatory Banking Capital, Estimation Error, and Systemic Risk in Ratings Based Capital Rules.

Scherer, Dominik; Kleinen, Pascal T.; Reher, Gerrit (2023): Statistical Uncertainty of PD Estimation under the Basel Regulations.

Tasche, Dirk (2010): Estimating discriminatory power and PD curves when the number of defaults is small.

Vasicek, Oldrich Alfons (1987): Probability of Loss on Loan Portfolio.

Wosnitza, Jan Henrik (2023a): Calibration alternatives to logistic regression and their potential for transferring the statistical dispersion of discriminatory power into uncertainties in probabilities of default. In *Journal of Credit Risk* 19 (1), pp. 75–103. DOI: 10.21314/JCR.2022.005.

Wosnitza, Jan Henrik (2023b): Public consultation on the revised ECB guide to internal models. Available online at https://www.bankingsupervision.europa.eu/legalframework/publiccons/pdf/internal_models_202306/internal_models_comment19.en.pdf.

Wosnitza, Jan Henrik (2025): Variance Estimation for the Quantification of the Margin of Conservatism Category C. In *Journal of Credit Risk* 21 (3), pp. 75–104. DOI: 10.21314/JCR.2025.012.

Wunderer, Christoph (2019): Asset correlation estimation for inhomogeneous exposure pools. In *Journal of Credit Risk* 15 (3), pp. 1–19. Available online at https://doi.org/10.21314/JCR.2019.251.

Appendix A: Time dependency of the standard deviation

According to Paragraph 210 (a) of the EGIM, the European Central Bank expects that "the shorter the time series are, the higher the MoC [C] […] should be". Obviously, the factor $\left(1-\frac{143+3\cdot\Delta}{36\cdot T}\right)$ is a strictly monotonically increasing function of T. Therefore, the purpose of this appendix is to differentiate the T-dependent term of the equation for variance of the LRADR, given in the second-to-last line of Equation (C.1), with respect to T:

$$\begin{aligned}\frac{\partial}{\partial T}\frac{1-\frac{143+3\cdot\Delta}{36\cdot T}}{T} &= \frac{\partial}{\partial T}\left[\frac{1}{T}-\frac{143+3\cdot\Delta}{36\cdot T^2}\right]\\ &= -\frac{1}{T^2}+2\cdot\frac{143+3\cdot\Delta}{36\cdot T^3}\\ &= \frac{1}{T^2}\left(\frac{143+3\cdot\Delta}{18\cdot T}-1\right)\overset{T>\frac{143+3\cdot\Delta}{18}}{<}0\end{aligned} \tag{A.1}$$

Obviously, the variance of the LRADR is a strictly monotonically decreasing function of time for $\frac{143+3\cdot\Delta}{18\cdot T}-1<0 \Leftrightarrow T>\frac{143+3\cdot\Delta}{18}$ as expected by the European Central Bank.

Appendix B: Derivation of the calibration target level

This appendix presents a step-by-step derivation of Equation (3) as referenced in the main text.

$$
\begin{aligned}
\frac{1}{T}\cdot\sum_{t=1}^{T} DR_t &= \frac{1}{T}\cdot\sum_{t=1}^{T}\frac{1}{N_1}\cdot\sum_{\tau=0}^{11} D_{t+\tau} \\
&= \frac{1}{T\cdot N_1}\cdot\sum_{t=1}^{T}\sum_{\tau=0}^{11} D_{t+\tau} \\
&= \frac{1}{T\cdot N_1}\cdot\left[\sum_{t=1}^{11} t\cdot D_t + \sum_{t=12}^{T} 12\cdot D_t + \sum_{t=T+1}^{T+11}[(T+11)-(t-1)]\cdot D_t\right] \\
&= \frac{1}{\sqrt{T}}\cdot\left[\sum_{t=1}^{11}\frac{t}{\sqrt{T}\cdot N_1}\cdot D_t + \sum_{t=12}^{T}\frac{12}{\sqrt{T}\cdot N_1}\cdot D_t + \sum_{t=T+1}^{T+11}\frac{(T+11)-(t-1)}{\sqrt{T}\cdot N_1}\cdot D_t\right] \qquad \text{(B.1)} \\
&= \frac{1}{\sqrt{T}}\cdot\left[\sum_{t=1}^{11} a_t\cdot D_t + \sum_{t=12}^{T} a_t\cdot D_t + \sum_{t=T+1}^{T+11} a_t\cdot D_t\right] \\
&= \frac{1}{\sqrt{T}}\cdot\sum_{t=1}^{T+11} a_t\cdot D_t \\
&= \sum_{t=1}^{T+11}\frac{a_t}{\sqrt{T}}\cdot D_t,
\end{aligned}
$$

where $a_t = \begin{cases} \frac{t}{\sqrt{T}\cdot N_1} \text{ for } 1 \le t \le 11 \\ \frac{12}{\sqrt{T}\cdot N_1} \text{ for } 12 \le t \le T \\ \frac{(T+11)-(t-1)}{\sqrt{T}\cdot N_1} \text{ for } T+1 \le t \le T+11 \end{cases}$.

Appendix C: Approximation of variance of the long run average default rate in the case of overlapping one-year default rates

This appendix provides a detailed derivation of the approximate variance of the long run average default rate (LRADR) in the case of overlapping one-year default rates, given in Equation (4).

$$
\begin{aligned}
\mathbb{V}\left[\frac{1}{T}\cdot\sum_{t=1}^{T} DR_t\right] &\overset{(A)}{=} \mathbb{V}\left[\sum_{t=1}^{T+11}\frac{a_t}{\sqrt{T}}\cdot D_t\right] \\
&\overset{(B)}{=} \sum_{t=1}^{T+11}\mathbb{V}\left[\frac{a_t}{\sqrt{T}}\cdot D_t\right] + \sum_{t=1}^{T+11}\sum_{\substack{\tau=1\\ \tau\neq t}}^{T+11}\mathbb{Cov}\left[\frac{a_t}{\sqrt{T}}\cdot D_t,\frac{a_\tau}{\sqrt{T}}\cdot D_\tau\right] \\
&= \sum_{t=1}^{T+11}\frac{a_t^2}{T}\cdot\mathbb{V}[D_t] + \sum_{t=1}^{T+11}\sum_{\substack{\tau=1\\ \tau\neq t}}^{T+11}\frac{a_t\cdot a_\tau}{T}\cdot\mathbb{Cov}[D_t,D_\tau] \\
&\overset{(C)}{=} \sum_{t=1}^{T+11}\frac{a_t^2}{T}\cdot\mathbb{V}[D_t] + 2\cdot\sum_{t=2}^{T+11}\sum_{\tau=1}^{t-1}\frac{a_t\cdot a_\tau}{T}\cdot\mathbb{Cov}[D_t,D_\tau] \\
&\overset{(D)}{=} \sum_{t=1}^{T+11}\frac{a_t^2}{T}\cdot\mathbb{V}[D_t] + 2\cdot\left[\sum_{t=2}^{T+11}\frac{a_t\cdot a_{t-1}}{T}\cdot\mathbb{Cov}[D_t,D_{t-1}] + \sum_{t=3}^{T+11}\frac{a_t\cdot a_{t-2}}{T}\cdot\mathbb{Cov}[D_t,D_{t-2}] + \cdots + \sum_{t=T+11}^{T+11}\frac{a_t\cdot a_{t-(T+10)}}{T}\cdot\mathbb{Cov}\left[D_t,D_{t-(T+10)}\right]\right] \qquad \text{(C.1)} \\
&= \sum_{t=1}^{T+11}\frac{a_t^2}{T}\cdot\mathbb{V}[D_t] + 2\cdot\sum_{\Delta=1}^{T}\sum_{t=\Delta+1}^{T+11}\frac{a_t\cdot a_{t-\Delta}}{T}\cdot\mathbb{Cov}[D_t,D_{t-\Delta}] \\
&\overset{(E)}{=} \frac{\mathbb{V}[D_t]}{T}\cdot\sum_{t=1}^{T+11}a_t^2 + 2\cdot\sum_{\Delta=1}^{T}\frac{\mathbb{Cov}[D_t,D_{t-\Delta}]}{T}\cdot\sum_{t=\Delta+1}^{T+11}a_t\cdot a_{t-\Delta} \\
&\overset{(F)}{=} \frac{\mathbb{V}[D_t]}{T\cdot N_1^2}\cdot 12^2\cdot\left(1-\frac{143}{36\cdot T}\right) + 2\cdot\sum_{\Delta=1}^{T}\frac{\mathbb{Cov}[D_t,D_{t-\Delta}]}{T\cdot N_1^2}\cdot 12^2\cdot\left(1-\frac{143+3\cdot\Delta}{36\cdot T}\right) \\
&= \frac{1}{T}\cdot\left(\frac{12}{N_1}\right)^2\cdot\left(\mathbb{V}[D_t]\cdot\left(1-\frac{143}{36\cdot T}\right) + 2\cdot\sum_{\Delta=1}^{T}\mathbb{Cov}[D_t,D_{t-\Delta}]\cdot\left(1-\frac{143+3\cdot\Delta}{36\cdot T}\right)\right) \\
&\overset{T\gg\frac{143+3\cdot\Delta}{36}}{\approx} \frac{1}{T}\cdot\left(\frac{12}{N_1}\right)^2\cdot\left(\mathbb{V}[D_t] + 2\cdot\sum_{\Delta=1}^{T}\mathbb{Cov}[D_t,D_{t-\Delta}]\right),
\end{aligned}
$$

where we

(A) apply the relationship $\frac{1}{T} \cdot \sum_{t=1}^{T} DR_t = \sum_{t=1}^{T+11} \frac{a_t}{\sqrt{T}} \cdot D_t$ from Equation (3),

(B) utilize (1) of the Appendix of Wosnitza (2025),

(C) use (2) of the Appendix of Wosnitza (2025),

(D) expand the sum to show all terms explicitly,

(E) assume for tractability that the Δ-lag covariance, $\mathbb{Cov}[D_t, D_{t-\Delta}]$, does not depend on t.

(F) apply the result $\sum_{t=\Delta+1}^{T+11} a_t \cdot a_{t-\Delta} = \frac{12^2}{N_1^2} \cdot \left\{1 - \frac{143+3\cdot\Delta}{36\cdot T}\right\}$ of Appendix D.

Appendix D: Derivation of the Sum of Products of Lagged Coefficients

The purpose of this appendix is to derive in detail the relationship $\sum_{t=\Delta+1}^{T+11} a_t \cdot a_{t-\Delta} = \frac{12}{T \cdot N_1^2} \cdot \left\{12 \cdot T - \frac{143}{3} - \Delta\right\}$ that we use in step (F) of the derivation of the variance of the LRADR in Appendix C. To this end, we make use of the standard summation formulas $\sum_{t=1}^{T} t = \frac{T \cdot (T+1)}{2}$ and $\sum_{t=1}^{T} t^2 = \frac{T \cdot (T+1) \cdot (2 \cdot T+1)}{6}$.

$$\sum_{t=\Delta+1}^{T+11} a_t \cdot a_{t-\Delta} = \sum_{t=\Delta+1}^{11+\Delta} a_t \cdot a_{t-\Delta} + \sum_{t=12+\Delta}^{T} a_t \cdot a_{t-\Delta} \sum_{t=T+1}^{T+11} a_t \cdot a_{t-\Delta}$$

$$= \sum_{t=\Delta+1}^{11+\Delta} \frac{t}{\sqrt{T} \cdot N_1} \cdot \frac{t-\Delta}{\sqrt{T} \cdot N_1} + \sum_{t=12+\Delta}^{T} \frac{12}{\sqrt{T} \cdot N_1} \cdot \frac{12}{\sqrt{T} \cdot N_1} + \sum_{t=T+1}^{T+11} \frac{(T+11)-(t-1)}{\sqrt{T} \cdot N_1} \cdot \frac{(T+11)-\big(t-(\Delta+1)\big)}{\sqrt{T} \cdot N_1}$$

$$= \frac{1}{T \cdot N_1^2} \cdot \left\{\sum_{t=\Delta+1}^{11+\Delta} t \cdot (t-\Delta) + 144 \cdot [T-(12+\Delta)+1] + \sum_{t=T+1}^{T+11} [(T+11)-(t-1)] \cdot [(T+11)-(t-\Delta-1)]\right\}$$

$$= \frac{1}{T \cdot N_1^2} \cdot \left\{\sum_{t=\Delta+1}^{11+\Delta} t^2 - \Delta \cdot \sum_{t=\Delta+1}^{11+\Delta} t + 144 \cdot [T-(11+\Delta)] + \sum_{t=T+1}^{T+11} [(T+11)^2 - (T+11) \cdot (2 \cdot t - \Delta - 2) + (t-1) \cdot (t-\Delta-1)]\right\}$$

$$= \frac{1}{T \cdot N_1^2} \cdot \left\{\sum_{t=\Delta+1}^{11+\Delta} t^2 - \Delta \cdot \sum_{t=\Delta+1}^{11+\Delta} t + 144 \cdot T - 144 \cdot 11 - 144 \cdot \Delta + \sum_{t=T+1}^{T+11} (T+11)^2 - (T+11) \cdot \sum_{t=T+1}^{T+11} (2 \cdot t - \Delta - 2) + \sum_{t=T+1}^{T+11} (t-1) \cdot (t-\Delta-1)\right\}$$

$$= \frac{1}{T \cdot N_1^2} \cdot \left\{\sum_{t=\Delta+1}^{11+\Delta} t^2 - \Delta \cdot \sum_{t=\Delta+1}^{11+\Delta} t + 144 \cdot T - 1584 - 144 \cdot \Delta + (T+11)^2 \cdot \sum_{t=T+1}^{T+11} 1 - (T+11) \cdot \left[2 \cdot \sum_{t=T+1}^{T+11} t - \sum_{t=T+1}^{T+11} (\Delta+2)\right] + \sum_{t=T+1}^{T+11} \big(t^2 - t \cdot (\Delta+1) - t + (\Delta+1)\big)\right\}$$

$$= \frac{1}{T \cdot N_1^2} \cdot \left\{\sum_{t=\Delta+1}^{11+\Delta} t^2 - \Delta \cdot \sum_{t=\Delta+1}^{11+\Delta} t + 144 \cdot T - 1584 - 144 \cdot \Delta + (T+11)^2 \cdot 11 - (T+11) \cdot \left[2 \cdot \sum_{t=T+1}^{T+11} t - (\Delta+2) \cdot \sum_{t=T+1}^{T+11} 1\right] + \sum_{t=T+1}^{T+11} t^2 - (\Delta+2) \cdot \sum_{t=T+1}^{T+11} t + (\Delta+1) \cdot \sum_{t=T+1}^{T+11} 1\right\}$$

$$= \frac{1}{T \cdot N_1^2} \cdot \left\{\sum_{t=\Delta+1}^{11+\Delta} t^2 - \Delta \cdot \sum_{t=\Delta+1}^{11+\Delta} t + 144 \cdot T - 1584 - 144 \cdot \Delta + (T+11)^2 \cdot 11 - (T+11) \cdot \left[2 \cdot \sum_{t=T+1}^{T+11} t - (\Delta+2) \cdot 11\right] + \sum_{t=T+1}^{T+11} t^2 - (\Delta+2) \cdot \sum_{t=T+1}^{T+11} t + (\Delta+1) \cdot 11\right\}$$

$$= \frac{1}{T \cdot N_1^2} \cdot \left\{ \frac{(11 + \Delta) \cdot (11 + \Delta + 1) \cdot (2 \cdot (11 + \Delta) + 1)}{6} - \frac{\Delta \cdot (\Delta + 1) \cdot (2 \cdot \Delta + 1)}{6} - \Delta \cdot \left[\frac{(11 + \Delta) \cdot (12 + \Delta)}{2} - \frac{\Delta \cdot (\Delta + 1)}{2} \right] + 144 \cdot T - 1584 - 144 \cdot \Delta + (T + 11)^2 \cdot 11 \right.$$

$$- (T + 11) \cdot [(T + 11) \cdot (T + 12) - T \cdot (T + 1) - (\Delta + 2) \cdot 11] + \frac{(T + 11) \cdot (T + 12) \cdot (2 \cdot T + 23)}{6} - \frac{T \cdot (T + 1) \cdot (2 \cdot T + 1)}{6} - (\Delta + 2)$$

$$\left. \cdot \left[\frac{(T + 11) \cdot (T + 12)}{2} - \frac{T \cdot (T + 1)}{2} \right] + (\Delta + 1) \cdot 11 \right\}$$

$$= \frac{1}{T \cdot N_1^2} \cdot \left\{ \frac{(132 + 23 \cdot \Delta + \Delta^2) \cdot (23 + 2 \cdot \Delta)}{6} - \frac{\Delta \cdot (2 \cdot \Delta^2 + 3 \cdot \Delta + 1)}{6} - \Delta \cdot \left[\frac{132 + 23 \cdot \Delta + \Delta^2}{2} - \frac{\Delta^2 + \Delta}{2} \right] + 144 \cdot T - 1584 - 144 \cdot \Delta + (T + 11)^2 \cdot 11 - (T + 11) \right.$$

$$\cdot [T^2 + 23 \cdot T + 132 - T^2 - T - (\Delta + 2) \cdot 11] + \frac{(T^2 + 23 \cdot T + 132) \cdot (2 \cdot T + 23)}{6} - \frac{T \cdot (2 \cdot T^2 + 3 \cdot T + 1)}{6} - (\Delta + 2) \cdot \left[\frac{T^2 + 23 \cdot T + 132}{2} - \frac{T^2 + T}{2} \right]$$

$$\left. + (\Delta + 1) \cdot 11 \right\}$$

$$= \frac{1}{T \cdot N_1^2} \cdot \left\{ \frac{3036 + 264 \cdot \Delta + 529 \cdot \Delta + 46 \cdot \Delta^2 + 23 \cdot \Delta^2 + 2 \cdot \Delta^3}{6} - \frac{2 \cdot \Delta^3 + 3 \cdot \Delta^2 + \Delta}{6} - \Delta \cdot \left[\frac{132 + 22 \cdot \Delta}{2} \right] + 144 \cdot T - 1584 - 144 \cdot \Delta + (T + 11)^2 \cdot 11 - (T + 11) \right.$$

$$\left. \cdot [22 \cdot T + 132 - (\Delta + 2) \cdot 11] + \frac{2 \cdot T^3 + 23 \cdot T^2 + 46 \cdot T^2 + 529 \cdot T + 264 \cdot T + 3036}{6} - \frac{2 \cdot T^3 + 3 \cdot T^2 + T}{6} - (\Delta + 2) \cdot \left[\frac{22 \cdot T + 132}{2} \right] + (\Delta + 1) \cdot 11 \right\}$$

$$= \frac{1}{T \cdot N_1^2} \cdot \left\{ \frac{3036 + 792 \cdot \Delta + 66 \cdot \Delta^2}{6} - \Delta \cdot [11 \cdot \Delta + 66] + 144 \cdot T - 1584 - 144 \cdot \Delta + (T + 11)^2 \cdot 11 - (T + 11) \cdot [22 \cdot T + 132 - (\Delta + 2) \cdot 11] \right.$$

$$\left. + \frac{66 \cdot T^2 + 792 \cdot T + 3036}{6} - (\Delta + 2) \cdot [11 \cdot T + 66] + (\Delta + 1) \cdot 11 \right\}$$

$$= \frac{1}{T \cdot N_1^2} \cdot \{506 + 132 \cdot \Delta + 11 \cdot \Delta^2 - [11 \cdot \Delta^2 + 66 \cdot \Delta] + 144 \cdot T - 1584 - 144 \cdot \Delta + (T + 11)^2 \cdot 11 - (T + 11) \cdot [22 \cdot T + 132 - 11 \cdot \Delta - 22] + 506 + 132 \cdot T + 11 \cdot T^2$$

$$- (\Delta + 2) \cdot [11 \cdot T + 66] + 11 \cdot \Delta + 11\}$$

$$= \frac{1}{T \cdot N_1^2} \cdot \{506 + 132 \cdot \Delta + 11 \cdot \Delta^2 - 11 \cdot \Delta^2 - 66 \cdot \Delta + 144 \cdot T - 1584 - 144 \cdot \Delta + (T + 11)^2 \cdot 11 - (T + 11) \cdot [22 \cdot T + 110 - 11 \cdot \Delta - 22] + 506 + 132 \cdot T + 11 \cdot T^2$$

$$- 11 \cdot T \cdot \Delta - 66 \cdot \Delta - 22 \cdot T - 132 + 11 \cdot \Delta + 11\}$$

$$= \frac{1}{T \cdot N_1^2} \cdot \{-693 - 133 \cdot \Delta + 254 \cdot T + (T + 11)^2 \cdot 11 - (T + 11) \cdot [22 \cdot T + 110 - 11 \cdot \Delta] + 11 \cdot T^2 - 11 \cdot T \cdot \Delta\}$$

$$= \frac{1}{T \cdot N_1^2} \cdot \{-693 - 133 \cdot \Delta + 254 \cdot T + (T^2 + 22 \cdot T + 121) \cdot 11 - (22 \cdot T^2 + 110 \cdot T - 11 \cdot \Delta \cdot T + 242 \cdot T + 1210 - 121 \cdot \Delta) + 11 \cdot T^2 - 11 \cdot T \cdot \Delta\}$$

$$= \frac{1}{T \cdot N_1^2} \cdot \{-693 - 133 \cdot \Delta + 254 \cdot T + 11 \cdot T^2 + 242 \cdot T + 1331 - 22 \cdot T^2 - 110 \cdot T + 11 \cdot \Delta \cdot T - 242 \cdot T - 1210 + 121 \cdot \Delta + 11 \cdot T^2 - 11 \cdot T \cdot \Delta\}$$

$$= \frac{1}{T \cdot N_1^2} \cdot \{144 \cdot T - 572 - 12 \cdot \Delta\}$$

$$= \frac{12^2}{T \cdot N_1^2} \cdot \left\{T - \frac{143}{3} - \frac{\Delta}{12}\right\}$$

$$= \frac{12^2}{N_1^2} \cdot \left\{1 - \frac{143 + 3 \cdot \Delta}{36 \cdot T}\right\}$$

Appendix E: Aggregation of best estimate PD and MoC C

The purpose of this appendix is to examine the aggregation of the best estimate PD (i.e., the PD excluding MoC C) and the MoC C at the calibration segment level, resulting in a conservative $\widetilde{PD}$ (i.e., the PD including MoC C). The linear logistic regression is a standard calibration methodology (see Wosnitza (2023a) and references therein). In the framework of the logistic regression, PD and $\widetilde{PD}$ of an obligor with credit score s are given as follows:

$$\begin{aligned}
\widetilde{PD}(s) &= \frac{1}{1+\exp\{-l(s)\}} \\
&= \frac{1}{1+\exp\left\{-f(s)-\ln\left\{\frac{P(Y=1)}{1-P(Y=1)}\right\}\right\}} \\
&= \frac{1}{1+\exp\left\{-f(s)-\ln\left\{\frac{LRADR+MoC}{1-LRADR-MoC}\right\}\right\}} \\
&= \frac{1}{1+\frac{1-LRADR-MoC}{LRADR+MoC}\cdot\exp\{-f(s)\}} \\
PD(s) &= \widetilde{PD}(s)\Big|_{MoC=0} \\
&= \frac{1}{1+\frac{1-LRADR}{LRADR}\cdot\exp\{-f(s)\}},
\end{aligned} \tag{E.1}$$

where

- we start from Equation (21) of Wosnitza (2023a) ,
- we substitute $f(s)=\frac{\alpha^2-1}{2\cdot\alpha^2\cdot\sigma^2}\cdot s^2-\frac{\mu\cdot(\alpha^2+1)}{\alpha^2\cdot\sigma^2}\cdot s-\ln\{\alpha\}+\frac{\mu^2\cdot(\alpha^2-1)}{2\cdot\alpha^2\cdot\sigma^2}$ in the second line, and
- $LRADR$ stands for the long run average default rate, which is the best estimate calibration target level.

In the second-to-last line of Equation (E.4), we have to express $\exp\{-f(s)\}$ as a function of $PD(s)$. To this end, we apply the following transformation:

$$\begin{aligned}
&\Leftrightarrow \frac{1}{PD(s)} = 1+\frac{1-LRADR}{LRADR}\cdot\exp\{-f(s)\} \\
&\Leftrightarrow \frac{1}{PD(s)}-1 = \frac{1-LRADR}{LRADR}\cdot\exp\{-f(s)\} \\
&\Leftrightarrow \exp\{-f(s)\} = \frac{1-PD(s)}{PD(s)}\cdot\frac{LRADR}{1-LRADR}.
\end{aligned} \tag{E.2}$$

Next, we develop the conservative $\widetilde{PD}(s)$ in a Taylor Series around $MoC=0$ up to the first order:

$$\widetilde{PD}(s) \approx \widetilde{PD}(s)\Big|_{MoC=0}+\frac{\partial}{\partial MoC}\widetilde{PD}(s)\Big|_{MoC=0}\cdot MoC. \tag{E.3}$$

To this end, we differentiate $\widetilde{PD}(s) = \frac{1}{1+\frac{1-LRADR-MoC}{LRADR+MoC}\cdot\exp\{-f(s)\}}$ with respect to MoC and then we evaluate this derivative at $MoC = 0$:

$$
\begin{aligned}
\left.\frac{\partial}{\partial MoC}\widetilde{PD}(s)\right|_{MoC=0} &= \left.\frac{\partial}{\partial MoC}\frac{1}{1+\frac{1-LRADR-MoC}{LRADR+MoC}\cdot\exp\{-f(s)\}}\right|_{MoC=0} \\
&= \left.\frac{0-\frac{-1}{(LRADR+MoC)^2}\cdot\exp\{-f(s)\}}{\left(1+\frac{1-LRADR-MoC}{LRADR+MoC}\cdot\exp\{-f(s)\}\right)^2}\right|_{MoC=0} \\
&= \left.\frac{\frac{1}{(LRADR+MoC)^2}\cdot\exp\{-f(s)\}}{\left(1+\frac{1-LRADR-MoC}{LRADR+MoC}\cdot\exp\{-f(s)\}\right)^2}\right|_{MoC=0} \\
&= \left.\widetilde{PD}(s)^2\cdot\frac{1}{(LRADR+MoC)^2}\cdot\exp\{-f(s)\}\right|_{MoC=0} \\
&= \left.\widetilde{PD}(s)^2\cdot\frac{1}{(LRADR+MoC)^2}\cdot\frac{1-PD(s)}{PD(s)}\cdot\frac{LRADR}{1-LRADR}\right|_{MoC=0} \\
&= \frac{PD(s)\cdot[1-PD(s)]}{LRADR\cdot[1-LRADR]},
\end{aligned}
\tag{E.4}
$$

where we substitute $\exp\{-f(s)\} = \frac{1-PD(s)}{PD(s)}\cdot\frac{LRADR}{1-LRADR}$ in the second-to-last line. Hence, Equation (E.3) is equal to the following:

$$
\begin{aligned}
\widetilde{PD}(s) &= PD(s) + \frac{PD(s)\cdot[1-PD(s)]}{LRADR\cdot[1-LRADR]}\cdot MoC \\
&= PD(s)\cdot\left(1+\frac{MoC}{LRADR}\cdot\frac{1-PD(s)}{1-LRADR}\right).
\end{aligned}
\tag{E.5}
$$

The sum of the LRADR plus the MoC C is an upper bound of the average conservative PD over all obligors $i \in \{1, \dots, n\}$:

$$
\begin{aligned}
&\frac{1}{n}\cdot\sum_i\left[PD(s_i)+\frac{PD(s_i)\cdot[1-PD(s_i)]}{LRADR\cdot[1-LRADR]}\cdot MoC\right]\\
&=\frac{1}{n}\cdot\sum_i PD(s_i)+\frac{1}{n}\cdot\sum_i\frac{PD(s_i)\cdot[1-PD(s_i)]}{LRADR\cdot[1-LRADR]}\cdot MoC\\
&=\frac{1}{n}\cdot\sum_i PD(s_i)+\frac{MoC}{LRADR\cdot[1-LRADR]}\cdot\frac{1}{n}\cdot\sum_i[PD(s_i)-PD(s_i)^2]\\
&=\frac{1}{n}\cdot\sum_i PD(s_i)+\frac{MoC}{LRADR\cdot[1-LRADR]}\cdot\left[\frac{1}{n}\cdot\sum_i PD(s_i)-\frac{1}{n}\cdot\sum_i PD(s_i)^2\right]\\
&\overset{(7)}{\leq}\frac{1}{n}\cdot\sum_i PD(s_i)+\frac{MoC}{LRADR\cdot[1-LRADR]}\cdot\left[\frac{1}{n}\cdot\sum_i PD(s_i)-\left(\frac{1}{n}\cdot\sum_i PD(s_i)\right)^2\right]\\
&=LRADR+\frac{MoC}{LRADR\cdot[1-LRADR]}\cdot[LRADR-LRADR^2]\\
&=LRADR+MoC,
\end{aligned}
\tag{E.6}
$$

where we apply (7) of the appendix of Wosnitza (2025): $-\left(\frac{1}{n}\cdot\sum_{i=1}^{n}PD(s_i)\right)^2\geq-\frac{1}{n}\cdot\sum_{i=1}^{n}PD(s_i)^2$. In the second-to-last line, we use the fact that the average of best estimate PDs "reflects the long-run average default rate" (see EBA/2017/16). More precisely, Table 1 of the EBA/GL/2017/16 clarifies that the average of the current PD estimates is equal to the LRADR in the case of calibration philosophy TTC B. In the case of calibration philosophy TTC C, the average of PD estimates over the entire historical observation period is equal to the LRADR.

In the following, we first assume that the rating grades associated with high PDs are, if at all, only scarcely populated. Second, we assume that both the PDs of the populated rating grades and the LRADR are small. For small $PD(s_i)$ and small $LRADR$, the product $\frac{PD(s_i)}{LRADR}\cdot\frac{1-PD(s_i)}{1-LRADR}$ converges towards $\frac{PD(s_i)}{LRADR}$ as shown in the following:[12]

$$
\begin{aligned}
PD(s_i)&=\frac{\alpha_i}{x}\\
LRADR&=\frac{1}{x}\\
\Rightarrow\frac{PD(s_i)}{LRADR}\cdot\frac{1-PD(s_i)}{1-LRADR}&=\frac{\frac{\alpha_i}{x}}{\frac{1}{x}}\cdot\frac{1-\frac{\alpha_i}{x}}{1-\frac{1}{x}}=\alpha_i\cdot\frac{x-\alpha_i}{x-1}\overset{x\gg\max\{\alpha_i;1\}}{\longrightarrow}\alpha_i=\frac{PD(s_i)}{LRADR}.
\end{aligned}
\tag{E.7}
$$

Distributing the MoC C at calibration segment level to the grades by scaling the MoC C at calibration segment with the ratio $\frac{PD(s_i)}{LRADR}$ yields two key benefits. First, the MoC C at grade level is proportional to the PD associated with the grade. This ensures that the MoC C of rating

[12] In our notation, the assumption of small PDs and small LRADR is equivalent to large x.

grades associated with low PDs is not extraordinarily high. Second, the average of the conservative PDs over all obligors i is equal to the sum of the LRADR plus the MoC C at calibration segment level:

$$\begin{aligned} \frac{1}{n}\cdot\sum_i\left[PD(s_i)+\frac{PD(s_i)}{LRADR}\cdot MoC\right] &= \frac{1}{n}\cdot\sum_i PD(s_i)+\frac{1}{n}\cdot\sum_i\frac{PD(s_i)}{LRADR}\cdot MoC \\ &= \frac{1}{n}\cdot\sum_i PD(s_i)+\frac{MoC}{LRADR}\cdot\frac{1}{n}\cdot\sum_i PD(s_i) \\ &= LRADR+\frac{MoC}{LRADR}\cdot LRADR \\ &= LRADR+MoC. \end{aligned} \tag{E.8}$$

That is why we propose to use $\left(1+\frac{MoC}{LRADR}\right)$ instead of $\left(1+\frac{MoC}{LRADR}\cdot\frac{1-PD(s)}{1-LRADR}\right)$ to break down the MoC C at calibration segment level to individual PDs. Finally, we replace $PD(s)$ and $\widetilde{PD}(s)$ in Equation (E.5) with PD_k and $\widetilde{PD}_k$, respectively, to adapt this result to the nomenclature used in Section 3:

$$\widetilde{PD}_k \approx PD_k+\underbrace{\frac{PD_k}{LRADR}}_{=\beta_k}\cdot MoC_k. \tag{E.9}$$

Appendix F: Differentiation of the risk weighted exposure amount

In this appendix, we provide a detailed derivation of Equation (7) obtained by differentiating $RWEA(MoC_k)$ with respect to MoC_k using the chain rule.

$$
\begin{aligned}
\Rightarrow \frac{\partial}{\partial MoC_k} RWEA(MoC_k) &= C_k \cdot \frac{\partial}{\partial MoC_k}\left\{\Phi\left[\frac{\Phi^{-1}(PD_k + \alpha \cdot \beta_k \cdot MoC_k) + a_k}{b_k}\right] - (PD_k + \alpha \cdot \beta_k \cdot MoC_k)\right\} \\
&= C_k \cdot \left\{\frac{\alpha \cdot \beta_k}{b_k} \cdot \frac{1}{\varphi[\Phi^{-1}(PD_k + \alpha \cdot \beta_k \cdot MoC_k)]} \cdot \varphi\left[\frac{\Phi^{-1}(PD_k + \alpha \cdot \beta_k \cdot MoC_k) + a_k}{b_k}\right] - \alpha \cdot \beta_k\right\} \\
&= \frac{\alpha \cdot \beta_k}{b_k} \cdot C_k \cdot \left\{\frac{1}{\varphi\left[\underbrace{\Phi^{-1}(PD_k + \alpha \cdot \beta_k \cdot MoC_k)}_{x_k}\right]} \cdot \varphi\left[\frac{\overbrace{\Phi^{-1}(PD_k + \alpha \cdot \beta_k \cdot MoC_k)}^{=x_k} + a_k}{b_k}\right] - b_k\right\} \\
&= \frac{\alpha \cdot \beta_k}{b_k} \cdot C_k \cdot \left\{\frac{\frac{1}{\sqrt{2 \cdot \pi}} \cdot \exp\left\{-\frac{1}{2} \cdot \left(\frac{x_k + a_k}{b_k}\right)^2\right\}}{\frac{1}{\sqrt{2 \cdot \pi}} \cdot \exp\left\{-\frac{1}{2} \cdot x^2\right\}} - b_k\right\} \\
&= \frac{\alpha \cdot \beta_k}{b_k} \cdot C_k \cdot \left\{\exp\left\{-\frac{1}{2} \cdot \left[\left(\frac{x_k + a_k}{b_k}\right)^2 - x_k^2\right]\right\} - b_k\right\} \\
&= \frac{\alpha \cdot \beta_k}{b_k} \cdot C_k \cdot \left\{\exp\left\{-\frac{1}{2} \cdot \left[\frac{x_k^2 + 2 \cdot a_k \cdot x_k + a_k^2}{b_k^2} - x^2\right]\right\} - b_k\right\} \\
&= \frac{\alpha \cdot \beta_k}{b_k} \cdot C_k \cdot \left\{\exp\left\{-\frac{1}{2} \cdot \left[\frac{x_k^2 \cdot (1 - b_k^2) + 2 \cdot a_k \cdot x_k + a_k^2}{b_k^2}\right]\right\} - b_k\right\} \\
&= \frac{\alpha \cdot \beta_k}{b_k} \cdot C_k \cdot \left\{\exp\left\{-\frac{1}{2} \cdot \frac{1 - b_k^2}{b_k^2}\left[x_k^2 + 2 \cdot x_k \cdot \frac{a_k}{1 - b_k^2} + \frac{a_k^2}{1 - b_k^2}\right]\right\} - b_k\right\} \\
&= \frac{\alpha \cdot \beta_k}{b_k} \cdot C_k \cdot \left\{\exp\left\{-\frac{1}{2} \cdot \frac{1 - b_k^2}{b_k^2}\left[\left(x_k + \frac{a_k}{1 - b_k^2}\right)^2 - \frac{a_k^2}{(1 - b_k^2)^2} + \frac{a_k^2 - a_k^2 \cdot b_k^2}{(1 - b_k^2)^2}\right]\right\} - b_k\right\} \\
&= \frac{\alpha \cdot \beta_k}{b_k} \cdot C_k \cdot \left\{\exp\left\{-\frac{1}{2} \cdot \frac{1 - b_k^2}{b_k^2}\left[\left(x_k + \frac{a_k}{1 - b_k^2}\right)^2 - \frac{a_k^2 \cdot b_k^2}{(1 - b_k^2)^2}\right]\right\} - b_k\right\} \\
&= \frac{\alpha \cdot \beta_k}{b_k} \cdot C_k \cdot \left\{\exp\left\{-\frac{1}{2} \cdot \frac{1 - b_k^2}{b_k^2} \cdot \left(x_k + \frac{a_k}{1 - b_k^2}\right)^2 + \frac{a_k^2}{2 \cdot (1 - b_k^2)}\right\} - b_k\right\}
\end{aligned}
\tag{F.1}
$$

Appendix G: Step-by-Step Substitution Leading to the derivative of RWEA with respect to $\boldsymbol{MoC_k}$

The purpose of this appendix is to outline the substitution steps leading to Equation (8) in detail and to present the resulting expression when $MoC_k = 0$. To this end, we resubstitute $a_k = \sqrt{R(PD_k)} \cdot \Phi^{-1}(99.9\%)$, $b_k = \sqrt{1 - R(PD_k)}$, $\beta_k = \frac{PD_k}{LRADR}$ and $x_k = \Phi^{-1}\left(PD_k + \alpha \cdot \overbrace{\frac{PD_k}{LRADR}}^{=\beta_k} \cdot MoC_k\right)$ one by one:

$$
\begin{aligned}
\frac{\partial}{\partial MoC_k} RWEA(MoC_k) &\overset{b_k^2 = 1 - R(PD_k)}{=} \frac{\alpha \cdot \beta_k}{\sqrt{1 - R(PD_k)}} \cdot C_k \cdot \left\{\exp\left\{-\frac{1}{2} \cdot \frac{R(PD_k)}{1 - R(PD_k)} \cdot \left(x_k + \frac{a_k}{R(PD_k)}\right)^2 + \frac{a_k^2}{2 \cdot R(PD_k)}\right\} - \sqrt{1 - R(PD_k)}\right\} \\
&\overset{a_k^2 = R(PD_k) \cdot \Phi^{-1}(99.9\%)^2}{=} \frac{\alpha \cdot \beta_k}{\sqrt{1 - R(PD_k)}} \cdot C_k \cdot \left\{\exp\left\{-\frac{1}{2} \cdot \frac{R(PD_k)}{1 - R(PD_k)} \cdot \left(x_k + \frac{\Phi^{-1}(99.9\%)}{\sqrt{R(PD_k)}}\right)^2 + \frac{\Phi^{-1}(99.9\%)^2}{2}\right\} - \sqrt{1 - R(PD_k)}\right\} \\
&\overset{x_k = \Phi^{-1}(PD_k + \alpha \cdot \beta_k \cdot MoC_k)}{=} \frac{\alpha \cdot \beta_k}{\sqrt{1 - R(PD_k)}} \cdot C_k \\
&\cdot \left\{\exp\left\{-\frac{1}{2} \cdot \frac{R(PD_k)}{1 - R(PD_k)} \cdot \left(\Phi^{-1}(PD_k + \alpha \cdot \beta_k \cdot MoC_k) + \frac{\Phi^{-1}(99.9\%)}{\sqrt{R(PD_k)}}\right)^2 + \frac{\Phi^{-1}(99.9\%)^2}{2}\right\} - \sqrt{1 - R(PD_k)}\right\} \\
&\overset{\beta_k = \frac{PD_k}{LRADR}}{=} \frac{\alpha \cdot \frac{PD_k}{LRADR}}{\sqrt{1 - R(PD_k)}} \cdot C_k \\
&\cdot \left\{\exp\left\{-\frac{1}{2} \cdot \frac{R(PD_k)}{1 - R(PD_k)} \cdot \left(\Phi^{-1}\left(PD_k + \alpha \cdot \frac{PD_k}{LRADR} \cdot MoC_k\right) + \frac{\Phi^{-1}(99.9\%)}{\sqrt{R(PD_k)}}\right)^2 + \frac{\Phi^{-1}(99.9\%)^2}{2}\right\} - \sqrt{1 - R(PD_k)}\right\}
\end{aligned}
\tag{G.1}
$$

$$
\Rightarrow \frac{\partial}{\partial MoC_k} RWEA(MoC_k)\bigg|_{MoC_k = 0} = \frac{\alpha \cdot \frac{PD_k}{LRADR}}{\sqrt{1 - R(PD_k)}} \cdot C_k \cdot \left[\exp\left\{-\frac{1}{2} \cdot \frac{R(PD_k)}{1 - R(PD_k)} \cdot \left(\Phi^{-1}(PD_k) + \frac{\Phi^{-1}(99.9\%)}{\sqrt{R(PD_k)}}\right)^2 + \frac{\Phi^{-1}(99.9\%)^2}{2}\right\} - \sqrt{1 - R(PD_k)}\right]
$$

Appendix H: Linearization of RWEA and determination of the scaling factor α

This appendix provides a detailed derivation of the linearization applied to both sides of Equation (6), leading to an explicit expression for the scaling factor α.

$$
\begin{aligned}
&\sum_k C_k \cdot \left\{RWEA(0) + \frac{\partial}{\partial MoC} RWEA(MoC)\Big|_{MoC=0} \cdot MoC\right\} \overset{!}{\approx} \sum_k C_k \cdot \left\{RWEA(0) + \frac{\partial}{\partial MoC_k} RWEA(MoC_k)\Big|_{MoC_k=0} \cdot MoC_k\right\} \\
&\Leftrightarrow \sum_k C_k \cdot RWEA(0) + \sum_k C_k \cdot \frac{\partial}{\partial MoC} RWEA(MoC)\Big|_{MoC=0} \cdot MoC \overset{!}{\approx} \sum_k C_k \cdot RWEA(0) + \sum_k C_k \cdot \frac{\partial}{\partial MoC_k} RWEA(MoC_k)\Big|_{MoC_k=0} \cdot MoC_k \\
&\Leftrightarrow \sum_k C_k \cdot \frac{\partial}{\partial MoC} RWEA(MoC)\Big|_{MoC=0} \cdot MoC \approx \sum_k C_k \cdot \frac{\partial}{\partial MoC_k} RWEA(MoC_k)\Big|_{MoC_k=0} \cdot MoC_k \\
&\Leftrightarrow \sum_k \frac{\frac{PD_k}{LRADR}}{\sqrt{1-R(PD_k)}} \cdot C_k \cdot \left[\exp\left\{-\frac{1}{2}\cdot\frac{R(PD_k)}{1-R(PD_k)}\cdot\left(\Phi^{-1}(PD_k)+\frac{\Phi^{-1}(99.9\%)}{\sqrt{R(PD_k)}}\right)^2 + \frac{\Phi^{-1}(99.9\%)^2}{2}\right\} - \sqrt{1-R(PD_k)}\right] \cdot MoC \\
&\qquad \approx \sum_k \frac{\alpha}{\sqrt{1-R(PD_k)}} \cdot C_k \cdot \left[\exp\left\{-\frac{1}{2}\cdot\frac{R(PD_k)}{1-R(PD_k)}\cdot\left(\Phi^{-1}(PD_k)+\frac{\Phi^{-1}(99.9\%)}{\sqrt{R(PD_k)}}\right)^2 + \frac{\Phi^{-1}(99.9\%)^2}{2}\right\} - \sqrt{1-R(PD_k)}\right] \cdot MoC_k \\
&\Leftrightarrow MoC \cdot \sum_k \overbrace{\frac{\frac{PD_k}{LRADR}}{\sqrt{1-R(PD_k)}} \cdot C_k \cdot \left\{\exp\left\{-\frac{1}{2}\cdot\frac{R(PD_k)}{1-R(PD_k)}\cdot\left(\Phi^{-1}(PD_k)+\frac{\Phi^{-1}(99.9\%)}{\sqrt{R(PD_k)}}\right)^2 + \frac{\Phi^{-1}(99.9\%)^2}{2}\right\} - \sqrt{1-R(PD_k)}\right\}}^{=\frac{PD_k}{LRADR}\cdot w_k} \\
&\qquad \approx \alpha \cdot \sum_k \underbrace{\frac{1}{\sqrt{1-R(PD_k)}} \cdot C_k \cdot \left\{\exp\left\{-\frac{1}{2}\cdot\frac{R(PD_k)}{1-R(PD_k)}\cdot\left(\Phi^{-1}(PD_k)+\frac{\Phi^{-1}(99.9\%)}{\sqrt{R(PD_k)}}\right)^2 + \frac{\Phi^{-1}(99.9\%)^2}{2}\right\} - \sqrt{1-R(PD_k)}\right\}}_{=w_k} \cdot MoC_k \\
&\Leftrightarrow MoC \cdot \sum_k \frac{PD_k}{LRADR} \cdot w_k \approx \alpha \cdot \sum_k w_k \cdot MoC_k \\
&\Leftrightarrow MoC \approx \alpha \cdot \sum_k \frac{w_k}{\sum_{k'} \frac{PD_{k'}}{LRADR} \cdot w_{k'}} \cdot MoC_k \\
&\Leftrightarrow \alpha \approx \frac{MoC}{\sum_k \frac{w_k}{\sum_{k'} \frac{PD_{k'}}{LRADR} \cdot w_{k'}} \cdot MoC_k} = \frac{\frac{MoC}{LRADR}}{\sum_k \frac{w_k}{\sum_{k'} PD_{k'} \cdot w_{k'}} \cdot MoC_k}
\end{aligned}
\tag{H.1}
$$

Appendix I: Differences between predefined and median estimated asset correlations

This appendix illustrates the difference between the predefined asset correlation and the median estimated asset correlation as a function of the preliminary (theoretical) discriminatory power and the predefined asset correlation across various unconditional PDs. To achieve this, we randomly sample systematic and idiosyncratic factors 100 times.

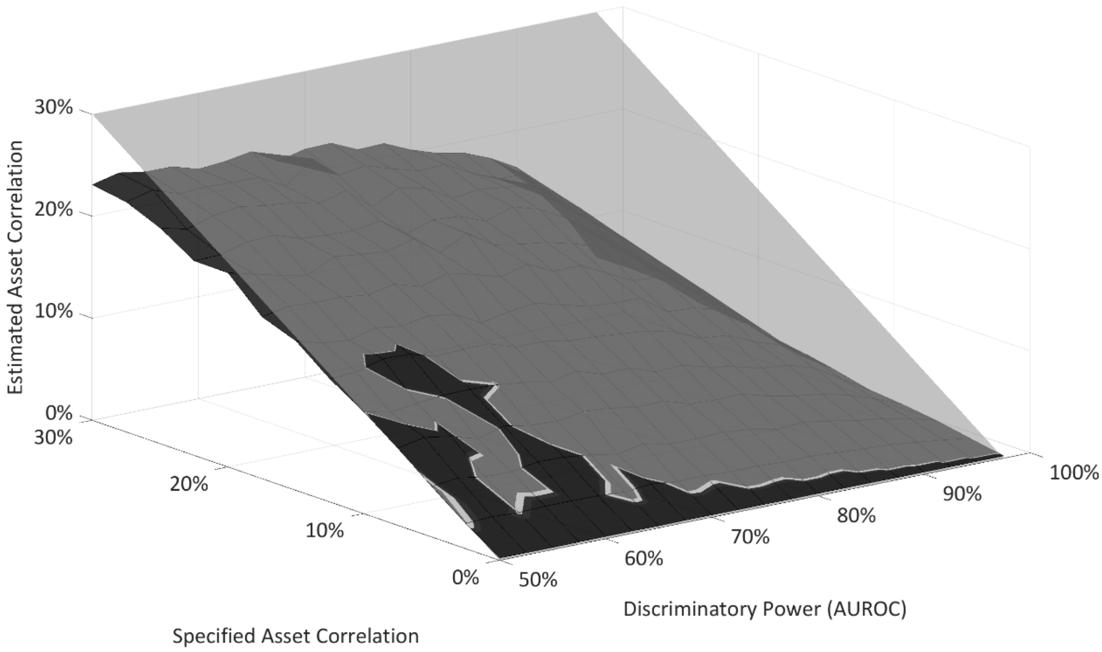

Figure 6: Comparison of theoretical (light grey surface) and median estimated (dark grey surface) asset correlation across 100 random draws of the systematic and idiosyncratic factors, shown as a function of the preliminary (theoretical) discriminatory power (measured by the AUROC) and predefined asset correlation. The unconditional PD is set to 0.5%. The figure illustrates that asset correlations estimated from time series of default rates (dark grey surface) tend to underestimate the predefined asset correlation (light grey surface). The extent of underestimation of the asset correlation varies with the preliminary (theoretical) discriminatory power (AUROC) and the true predefined asset correlation.

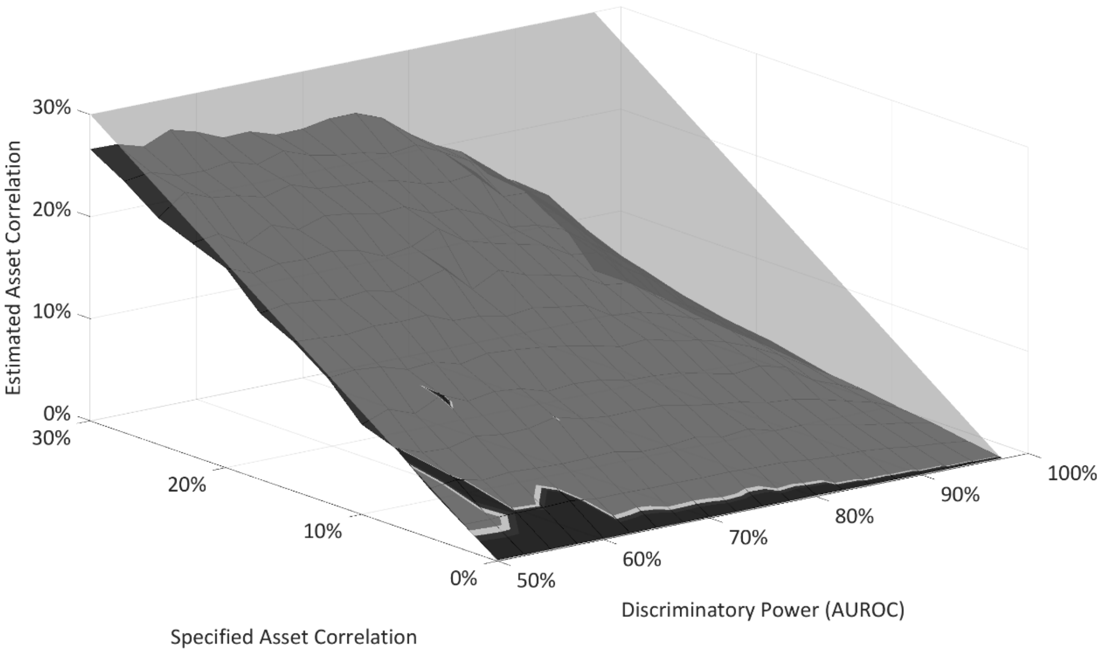

Figure 7: Comparison of theoretical (light grey surface) and median estimated (dark grey surface) asset correlation across 100 random draws of the systematic and idiosyncratic factors, shown as a function of the preliminary (theoretical) discriminatory power (measured by the AUROC) and predefined asset correlation. The unconditional PD is set to 1.0%. The figure illustrates that asset correlations estimated from time series of default rates (dark grey surface) tend to underestimate the predefined asset correlation (light grey surface). The extent of underestimation of the asset correlation varies with the preliminary (theoretical) discriminatory power (AUROC) and the true predefined asset correlation.

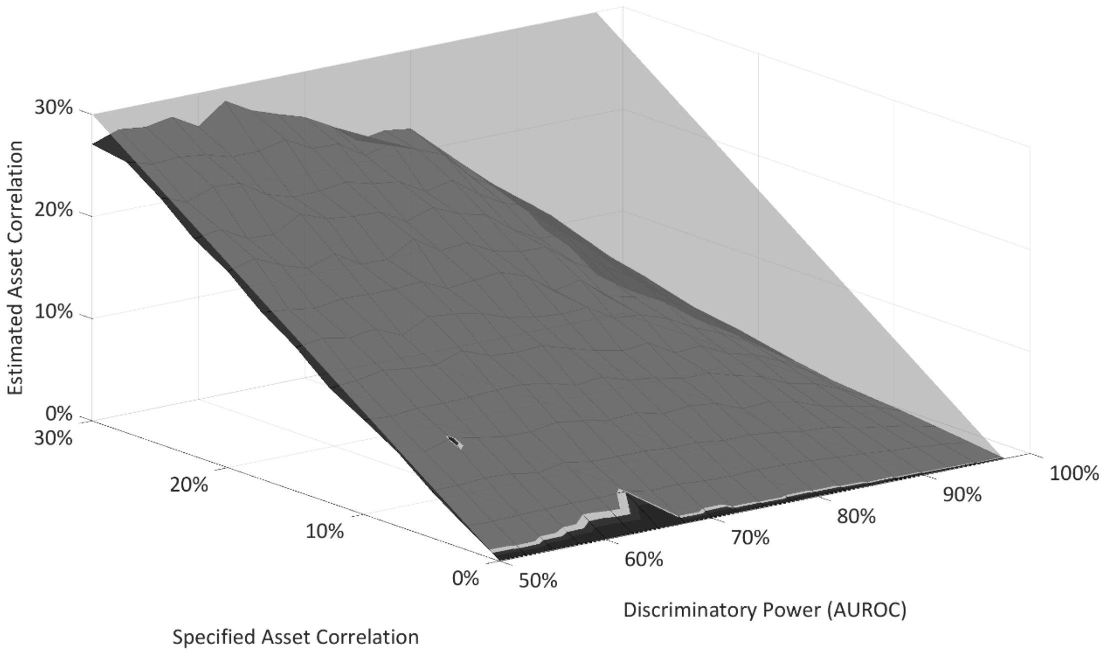

Figure 8: Comparison of theoretical (light grey surface) and median estimated (dark grey surface) asset correlation across 100 random draws of the systematic and idiosyncratic factors, shown as a function of the preliminary (theoretical) discriminatory power (measured by the AUROC) and predefined asset correlation. The unconditional PD is set to 2.0%. The figure illustrates that asset correlations estimated from time series of default rates (dark grey surface) tend to underestimate the predefined asset correlation (light grey surface). The extent of underestimation of the asset correlation varies with the preliminary (theoretical) discriminatory power (AUROC) and the true predefined asset correlation.

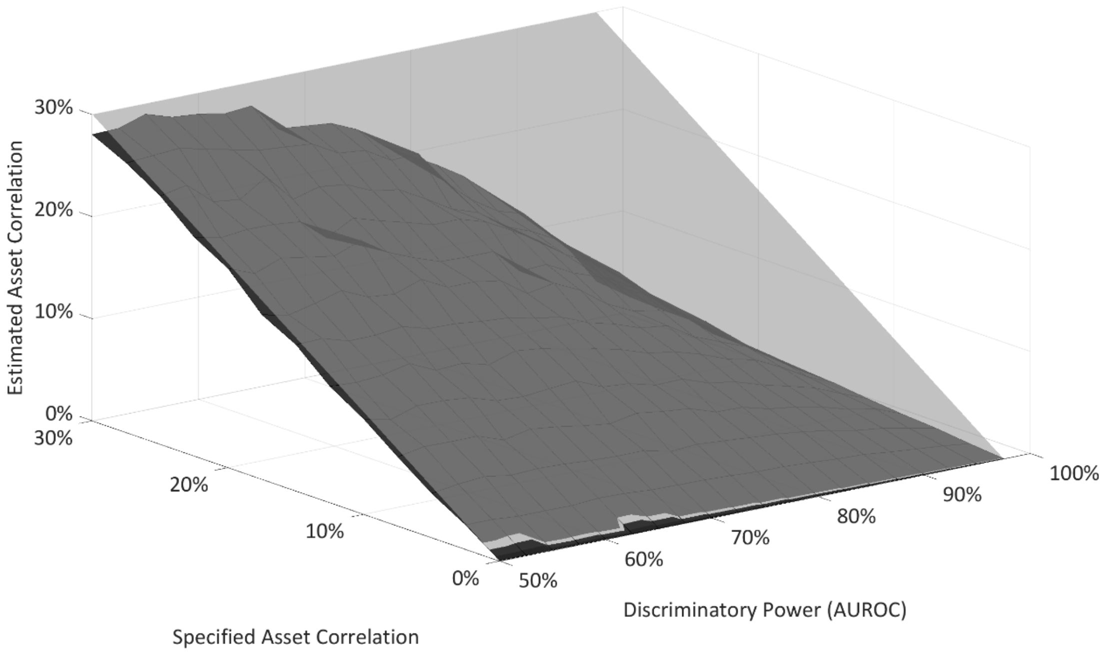

Figure 9: Comparison of theoretical (light grey surface) and median estimated (dark grey surface) asset correlation across 100 random draws of the systematic and idiosyncratic factors, shown as a function of the preliminary (theoretical) discriminatory power (measured by the AUROC) and predefined asset correlation. The unconditional PD is set to 4.0%. The figure illustrates that asset correlations estimated from time series of default rates (dark grey surface) tend to underestimate the predefined asset correlation (light grey surface). The extent of underestimation of the asset correlation varies with the preliminary (theoretical) discriminatory power (AUROC) and the true predefined asset correlation.

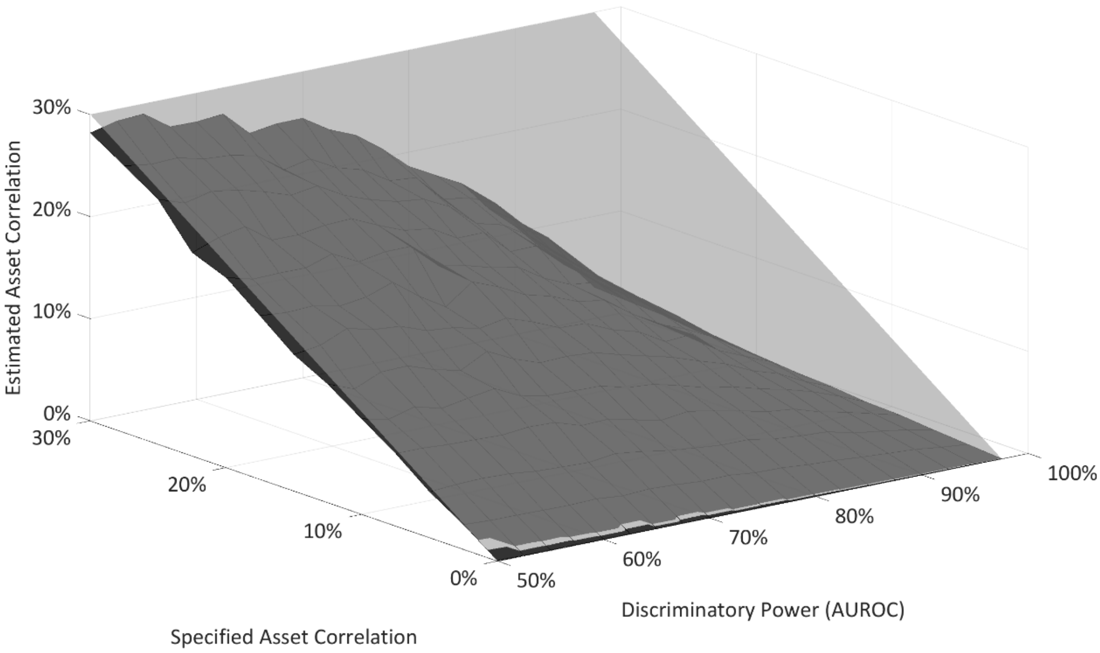

Figure 10: Comparison of theoretical (light grey surface) and median estimated (dark grey surface) asset correlation across 100 random draws of the systematic and idiosyncratic factors, shown as a function of the preliminary (theoretical) *discriminatory power (measured by the AUROC) and predefined asset correlation. The unconditional PD is set to 8.0%. The figure illustrates that asset correlations estimated from time series of default rates (dark grey surface) tend to underestimate the predefined asset correlation (light grey surface). The extent of underestimation of the asset correlation varies with the preliminary (theoretical) discriminatory power (AUROC) and the true predefined asset correlation.*

Appendix J: Comparison of estimated asset correlation using different empirical AUROC definitions

The purpose of this Appendix is to present plots of the estimated asset correlation as a function of both the final (empirical) AUROC and the true asset correlation for different unconditional PDs. The final (empirical) AUROC is defined in three ways.

- In Figure 11 to Figure 15, it is calculated as the average of the AUROC values calculated separately for each year within the 20-year historical observation period.
- In Figure 16 to Figure 20, it is calculated as the median of the AUROC values calculated separately for each year within the 20-year period.
- In Figure 21 to Figure 25, it is calculated from the pooled credit scores and default statuses over the entire 20-year period.

All of these figures are qualitatively very similar to those based on the preliminary (theoretical) discriminatory power (see Figure 1 to Figure 5).

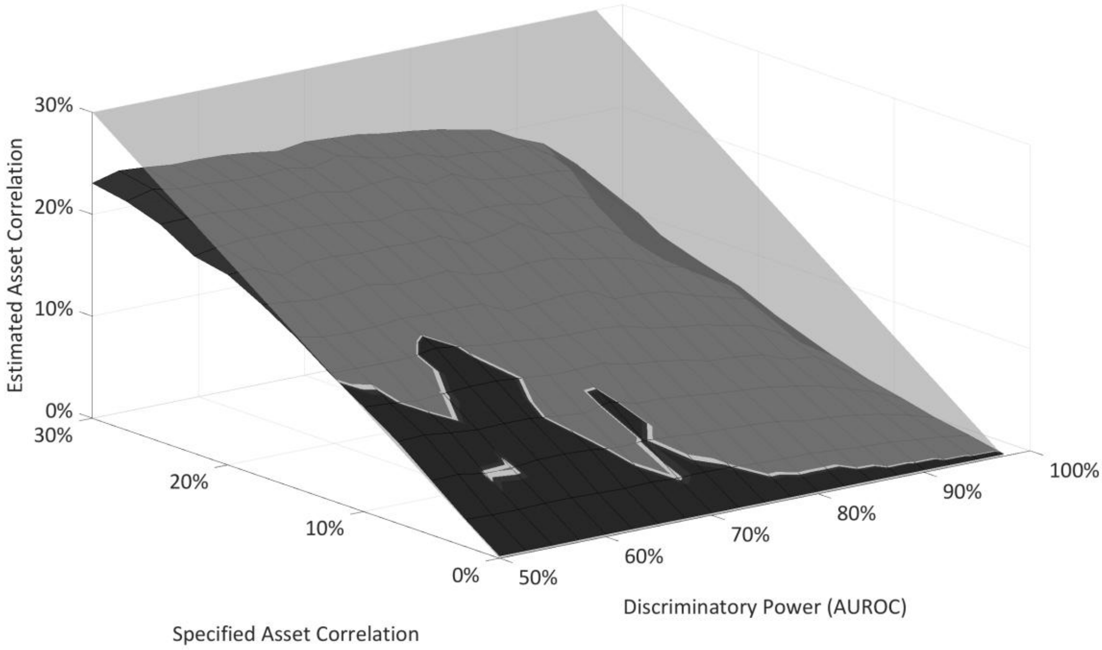

Figure 11: Comparison of theoretical (light grey surface) and average estimated (dark grey surface) asset correlation across 100 random draws of the systematic and idiosyncratic factors, shown as a function of the final (empirical) discriminatory power (measured by the average AUROC across the historical observation period) and predefined asset correlation. The unconditional PD is set to 0.5%. The figure illustrates that asset correlations estimated from time series of default rates (dark grey surface) tend to underestimate the predefined asset correlation (light grey surface). The extent of underestimation of the asset correlation varies with the final (empirical) discriminatory power (AUROC) and the true predefined asset correlation.

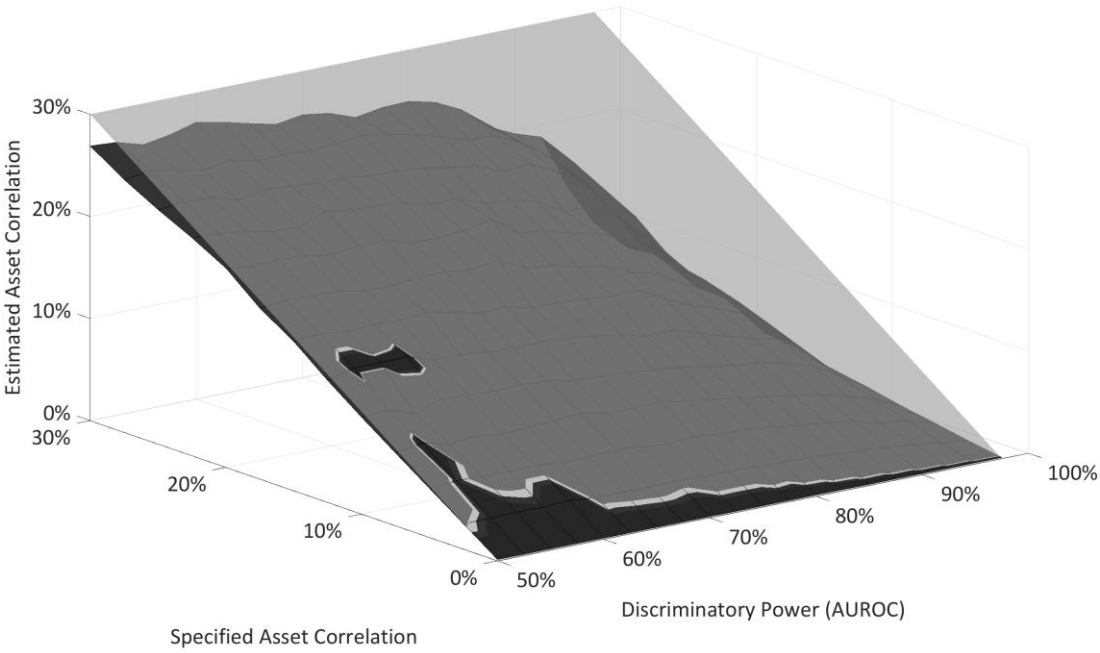

Figure 12: Comparison of theoretical (light grey surface) and average estimated (dark grey surface) asset correlation across 100 random draws of the systematic and idiosyncratic factors, shown as a function of the final (empirical) discriminatory power (measured by the average AUROC across the historical observation period) and predefined asset correlation. The unconditional PD is set to 1.0%. The figure illustrates that asset correlations estimated from time series of default rates (dark grey surface) tend to underestimate the predefined asset correlation (light grey surface). The extent of underestimation of the asset correlation varies with the final (empirical) discriminatory power (AUROC) and the true predefined asset correlation.

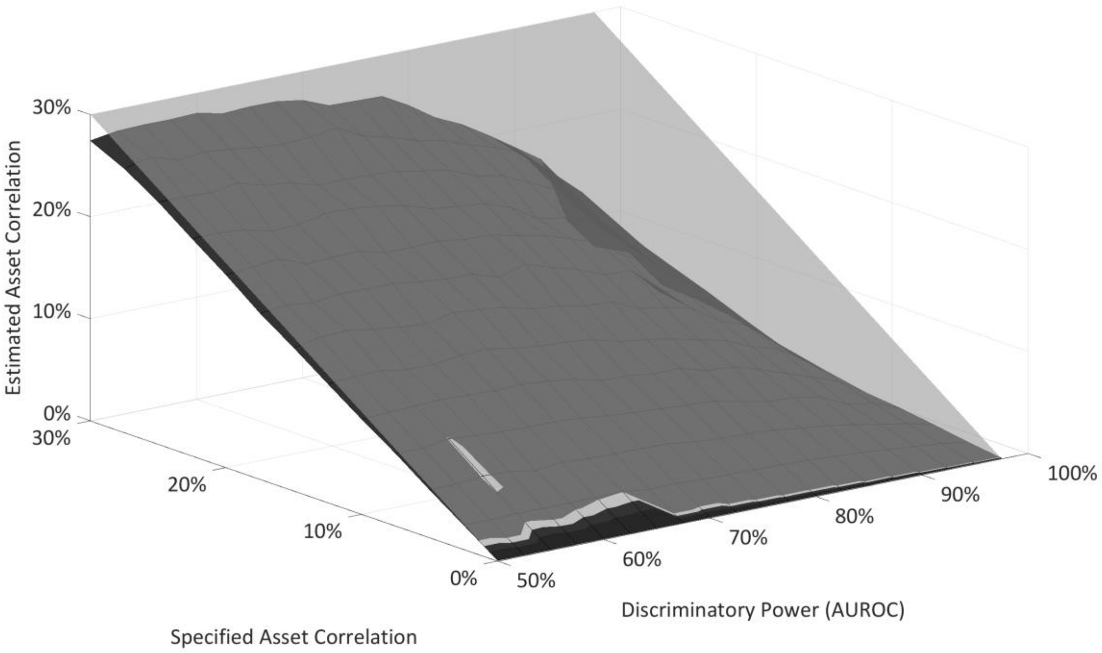

Figure 13: Comparison of theoretical (light grey surface) and average estimated (dark grey surface) asset correlation across 100 random draws of the systematic and idiosyncratic factors, shown as a function of the final (empirical) discriminatory power (measured by the average AUROC across the historical observation period) and predefined asset correlation. The unconditional PD is set to 2.0%. The figure illustrates that asset correlations estimated from time series of default rates (dark grey surface) tend to underestimate the predefined asset correlation (light grey surface). The extent of underestimation of the asset correlation varies with the final (empirical) discriminatory power (AUROC) and the true predefined asset correlation.

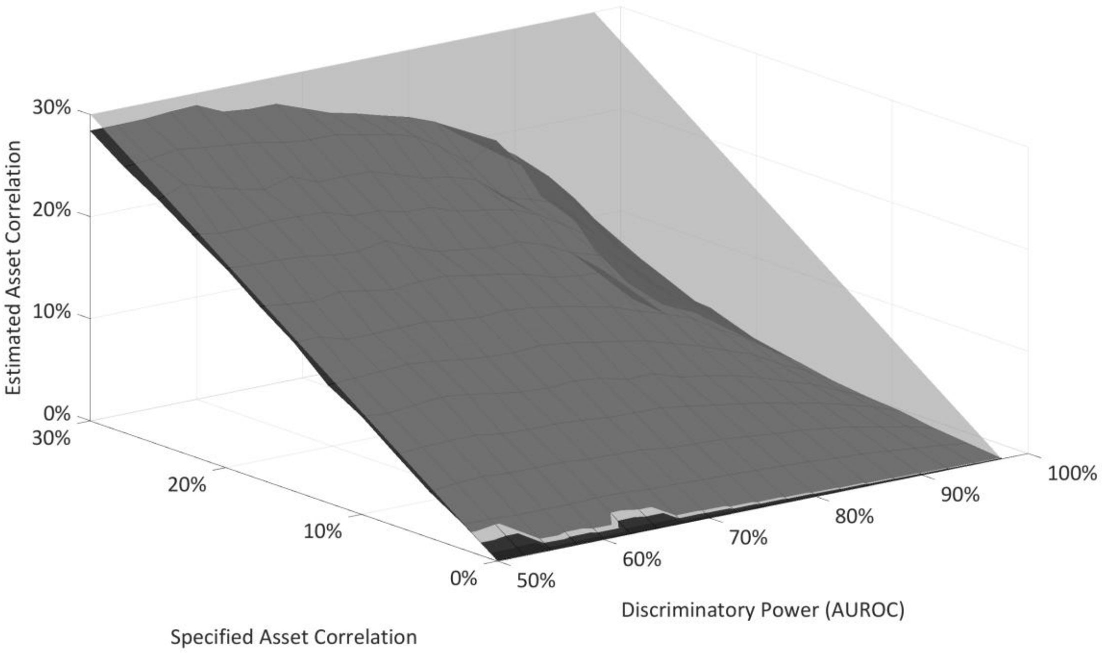

Figure 14: Comparison of theoretical (light grey surface) and average estimated (dark grey surface) asset correlation across 100 random draws of the systematic and idiosyncratic factors, shown as a function of the final (empirical) discriminatory power (measured by the average AUROC across the historical observation period) and predefined asset correlation. The unconditional PD is set to 4.0%. The figure illustrates that asset correlations estimated from time series of default rates (dark grey surface) tend to underestimate the predefined asset correlation (light grey surface). The extent of underestimation of the asset correlation varies with the final (empirical) discriminatory power (AUROC) and the true predefined asset correlation.

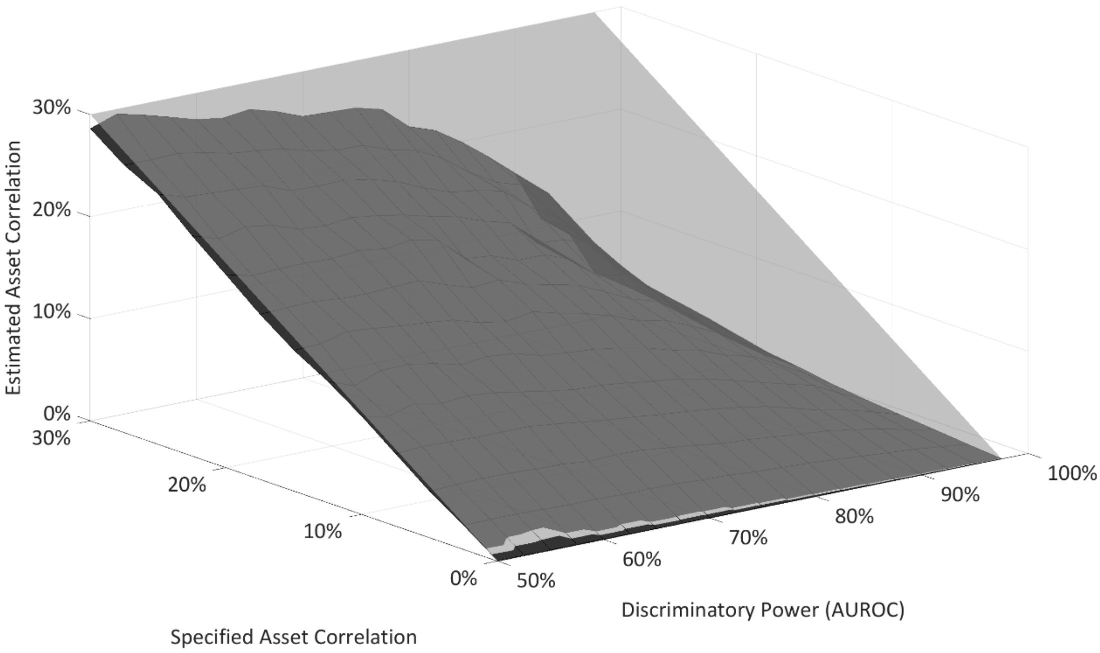

Figure 15: Comparison of theoretical (light grey surface) and average estimated (dark grey surface) asset correlation across 100 random draws of the systematic and idiosyncratic factors, shown as a function of the final (empirical) discriminatory power (measured by the average AUROC across the historical observation period) and predefined asset correlation. The unconditional PD is set to 8.0%. The figure illustrates that asset correlations estimated from time series of default rates (dark grey surface) tend to underestimate the predefined asset correlation (light grey surface). The extent of underestimation of the asset correlation varies with the final (empirical) discriminatory power (AUROC) and the true predefined asset correlation.

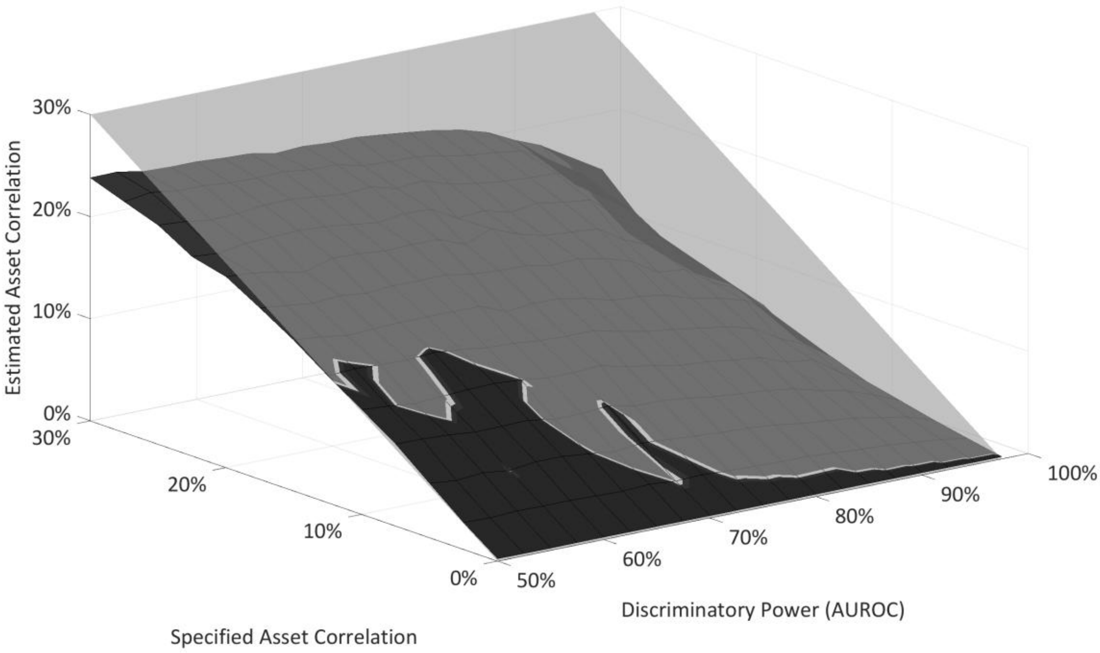

Figure 16: Comparison of theoretical (light grey surface) and average estimated (dark grey surface) asset correlation across 100 random draws of the systematic and idiosyncratic factors, shown as a function of the final (empirical) discriminatory power (measured by the median AUROC across the historical observation period) and predefined asset correlation. The unconditional PD is set to 0.5%. The figure illustrates that asset correlations estimated from time series of default rates (dark grey surface) tend to underestimate the predefined asset correlation (light grey surface). The extent of underestimation of the asset correlation varies with the final (empirical) discriminatory power (AUROC) and the true predefined asset correlation.

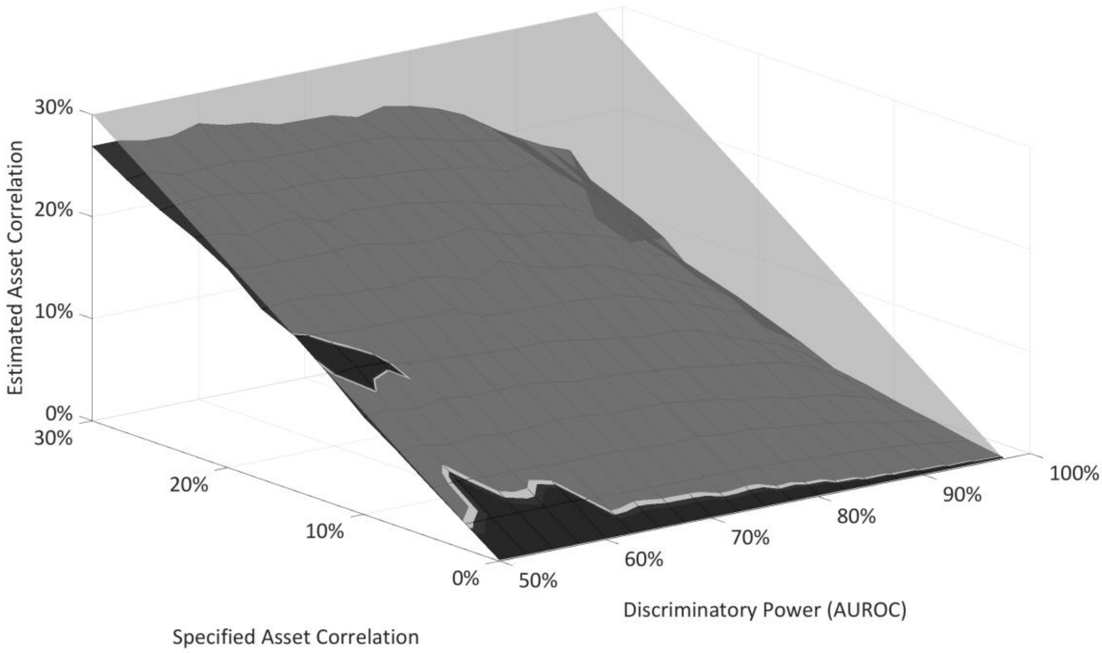

Figure 17: Comparison of theoretical (light grey surface) and average estimated (dark grey surface) asset correlation across 100 random draws of the systematic and idiosyncratic factors, shown as a function of the final (empirical) discriminatory power (measured by the median AUROC across the historical observation period) and predefined asset correlation. The unconditional PD is set to 1.0%. The figure illustrates that asset correlations estimated from time series of default rates (dark grey surface) tend to underestimate the predefined asset correlation (light grey surface). The extent of underestimation of the asset correlation varies with the final (empirical) discriminatory power (AUROC) and the true predefined asset correlation.

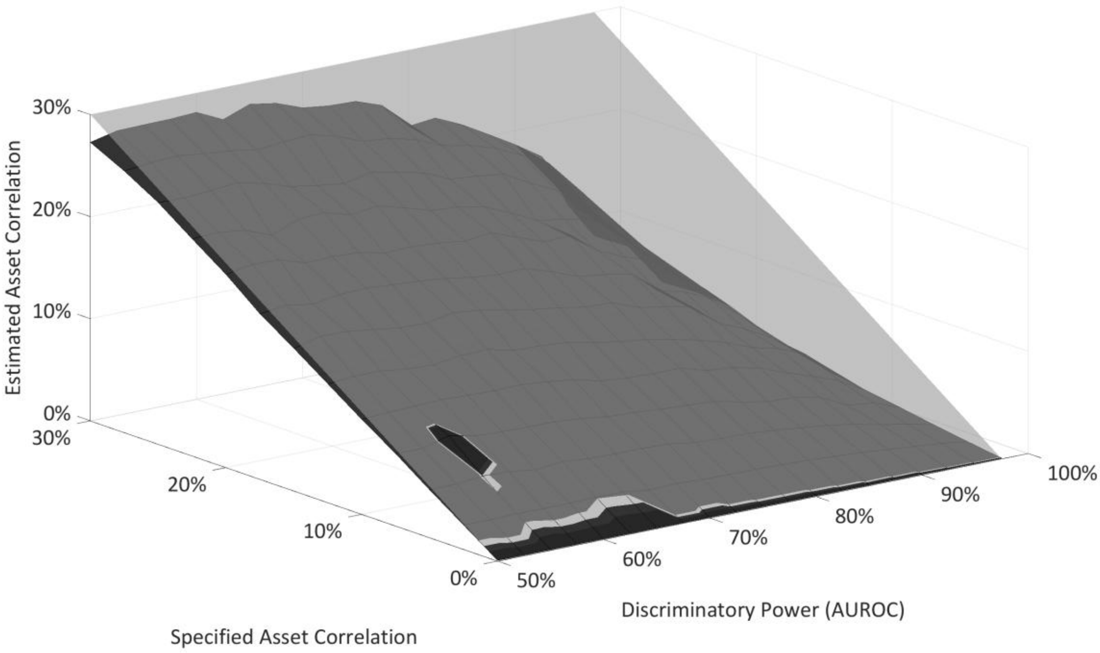

Figure 18: Comparison of theoretical (light grey surface) and average estimated (dark grey surface) asset correlation across 100 random draws of the systematic and idiosyncratic factors, shown as a function of the final (empirical) discriminatory power (measured by the median AUROC across the historical observation period) and predefined asset correlation. The unconditional PD is set to 2.0%. The figure illustrates that asset correlations estimated from time series of default rates (dark grey surface) tend to underestimate the predefined asset correlation (light grey surface). The extent of underestimation of the asset correlation varies with the final (empirical) discriminatory power (AUROC) and the true predefined asset correlation.

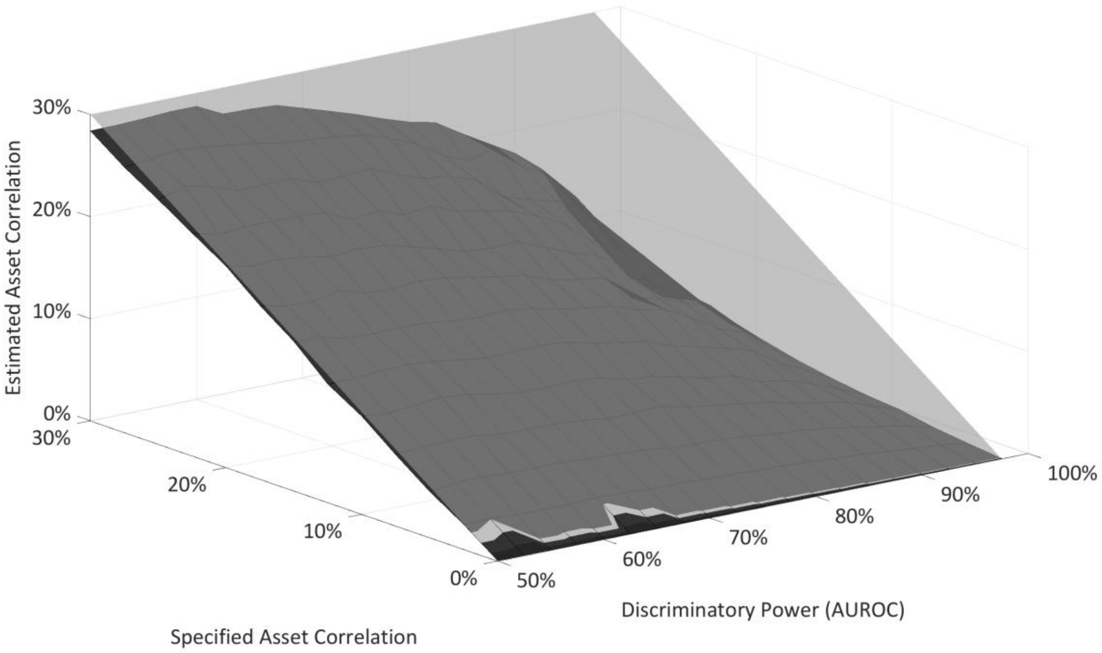

Figure 19: Comparison of theoretical (light grey surface) and average estimated (dark grey surface) asset correlation across 100 random draws of the systematic and idiosyncratic factors, shown as a function of the final (empirical) discriminatory power (measured by the median AUROC across the historical observation period) and predefined asset correlation. The unconditional PD is set to 4.0%. The figure illustrates that asset correlations estimated from time series of default rates (dark grey surface) tend to underestimate the predefined asset correlation (light grey surface). The extent of underestimation of the asset correlation varies with the final (empirical) discriminatory power (AUROC) and the true predefined asset correlation.

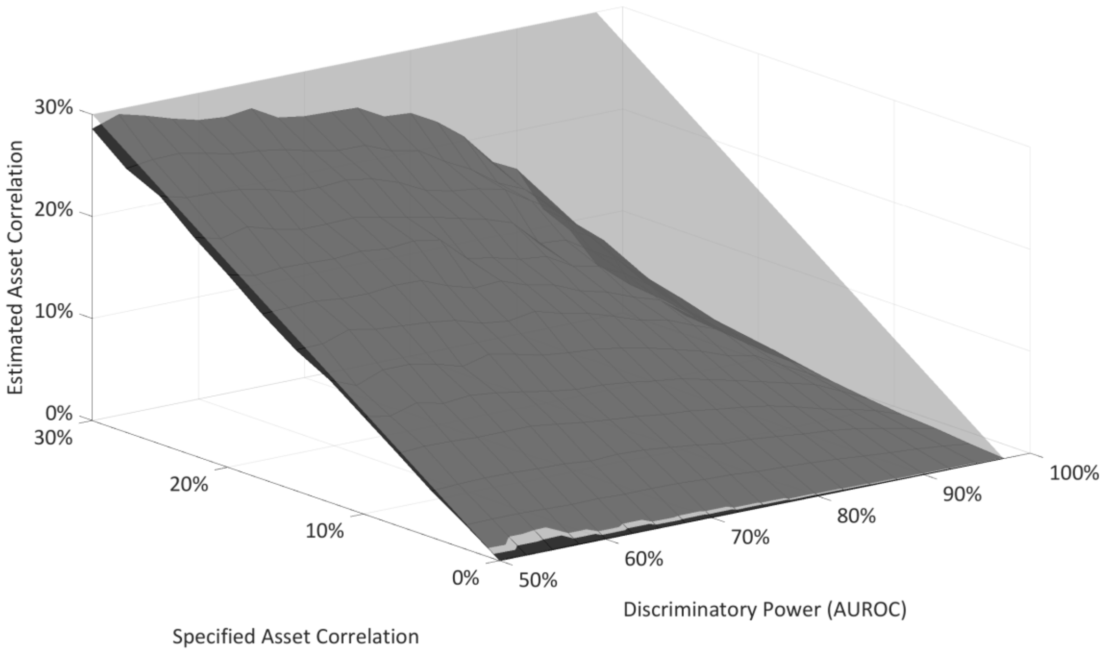

Figure 20: Comparison of theoretical (light grey surface) and average estimated (dark grey surface) asset correlation across 100 random draws of the systematic and idiosyncratic factors, shown as a function of the final (empirical) discriminatory power (measured by the median AUROC across the historical observation period) and predefined asset correlation. The unconditional PD is set to 8.0%. The figure illustrates that asset correlations estimated from time series of default rates (dark grey surface) tend to underestimate the predefined asset correlation (light grey surface). The extent of underestimation of the asset correlation varies with the final (empirical) discriminatory power (AUROC) and the true predefined asset correlation.

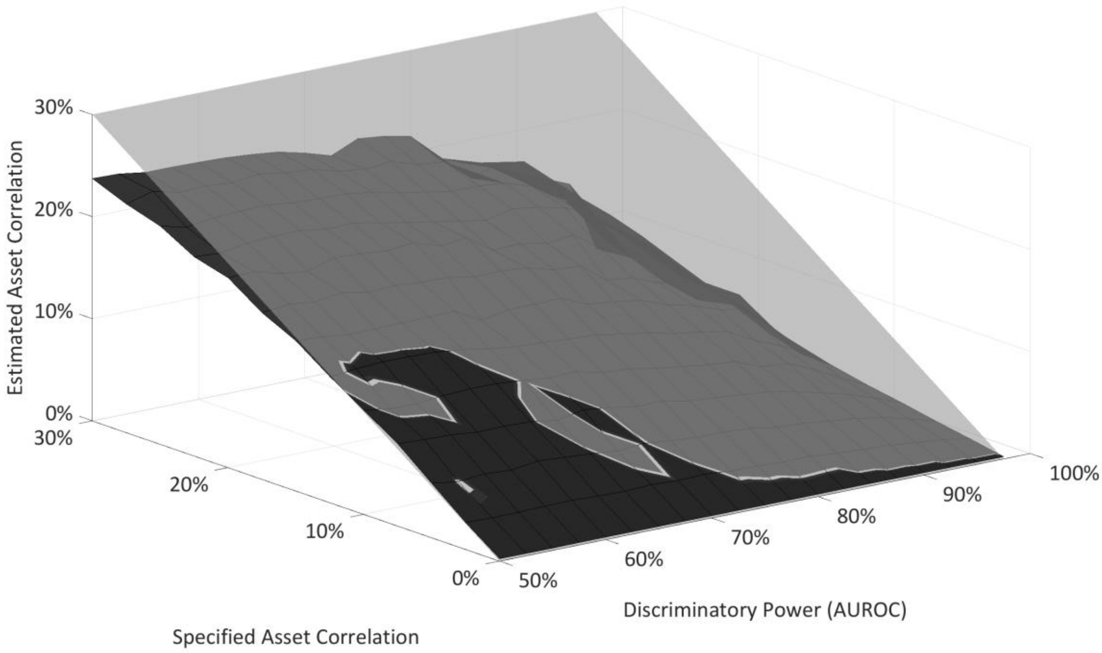

Figure 21: Comparison of theoretical (light grey surface) and average estimated (dark grey surface) asset correlation across 100 random draws of the systematic and idiosyncratic factors, shown as a function of the final (empirical) discriminatory power (measured by the AUROC calculated from the pooled dataset over the entire historical observation period) and predefined asset correlation. The unconditional PD is set to 0.5%. The figure illustrates that asset correlations estimated from time series of default rates (dark grey surface) tend to underestimate the predefined asset correlation (light grey surface). The extent of underestimation of the asset correlation varies with the final (empirical) discriminatory power (AUROC) and the true predefined asset correlation.

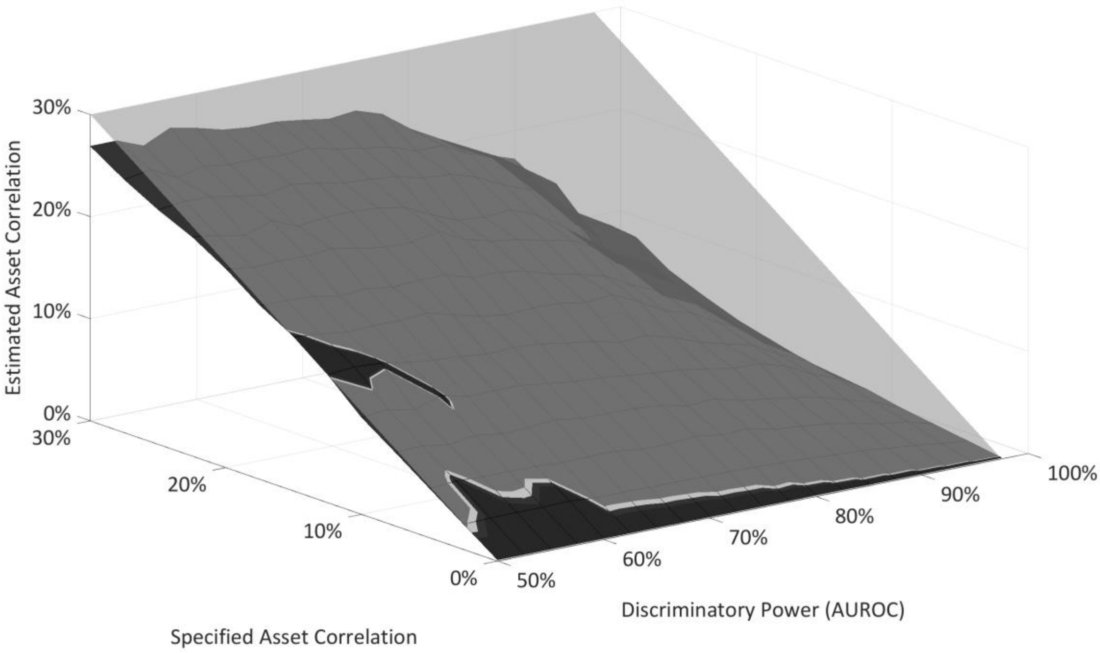

Figure 22: Comparison of theoretical (light grey surface) and average estimated (dark grey surface) asset correlation across 100 random draws of the systematic and idiosyncratic factors, shown as a function of the final (empirical) discriminatory power (measured by the AUROC calculated from the pooled dataset over the entire historical observation period) and predefined asset correlation. The unconditional PD is set to 1.0%. The figure illustrates that asset correlations estimated from time series of default rates (dark grey surface) tend to underestimate the predefined asset correlation (light grey surface). The extent of underestimation of the asset correlation varies with the final (empirical) discriminatory power (AUROC) and the true predefined asset correlation.

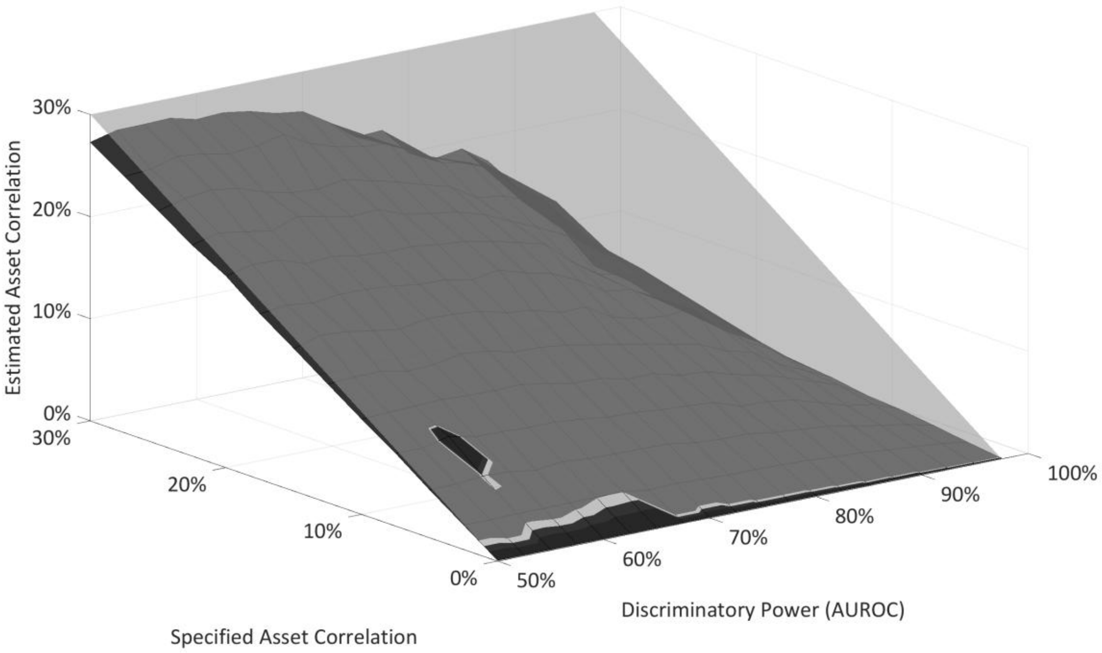

Figure 23: Comparison of theoretical (light grey surface) and average estimated (dark grey surface) asset correlation across 100 random draws of the systematic and idiosyncratic factors, shown as a function of the final (empirical) discriminatory power (measured by the AUROC calculated from the pooled dataset over the entire historical observation period) and predefined asset correlation. The unconditional PD is set to 2.0%. The figure illustrates that asset correlations estimated from time series of default rates (dark grey surface) tend to underestimate the predefined asset correlation (light grey surface). The extent of underestimation of the asset correlation varies with the final (empirical) discriminatory power (AUROC) and the true predefined asset correlation.

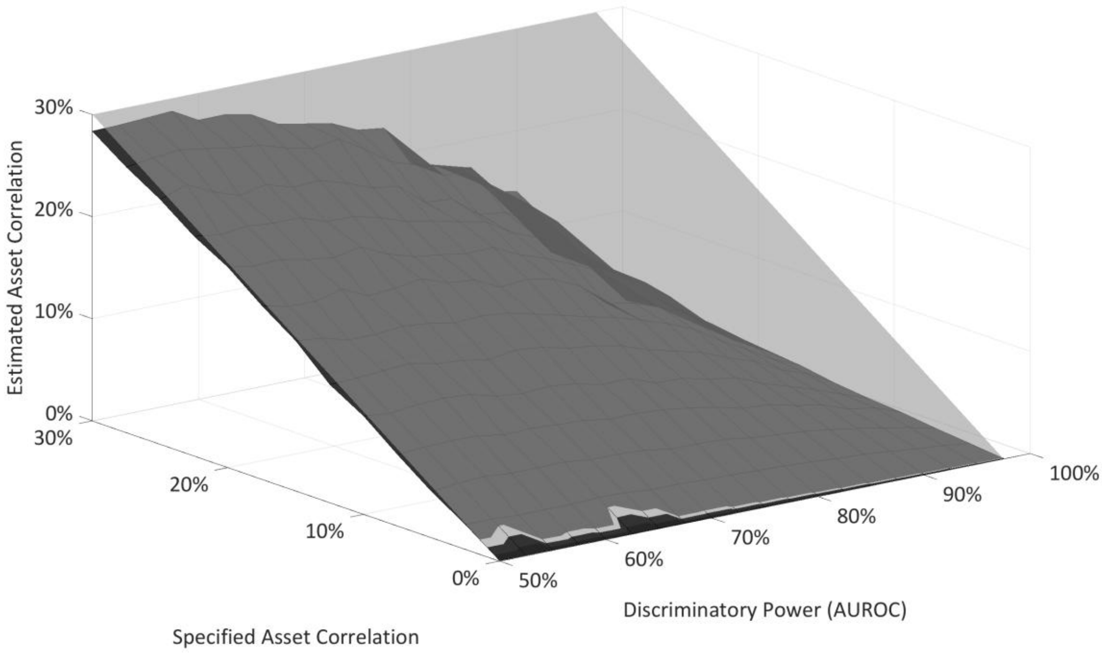

Figure 24: Comparison of theoretical (light grey surface) and average estimated (dark grey surface) asset correlation across 100 random draws of the systematic and idiosyncratic factors, shown as a function of the final (empirical) discriminatory power (measured by the AUROC calculated from the pooled dataset over the entire historical observation period) and predefined asset correlation. The unconditional PD is set to 4.0%. The figure illustrates that asset correlations estimated from time series of default rates (dark grey surface) tend to underestimate the predefined asset correlation (light grey surface). The extent of underestimation of the asset correlation varies with the final (empirical) discriminatory power (AUROC) and the true predefined asset correlation.

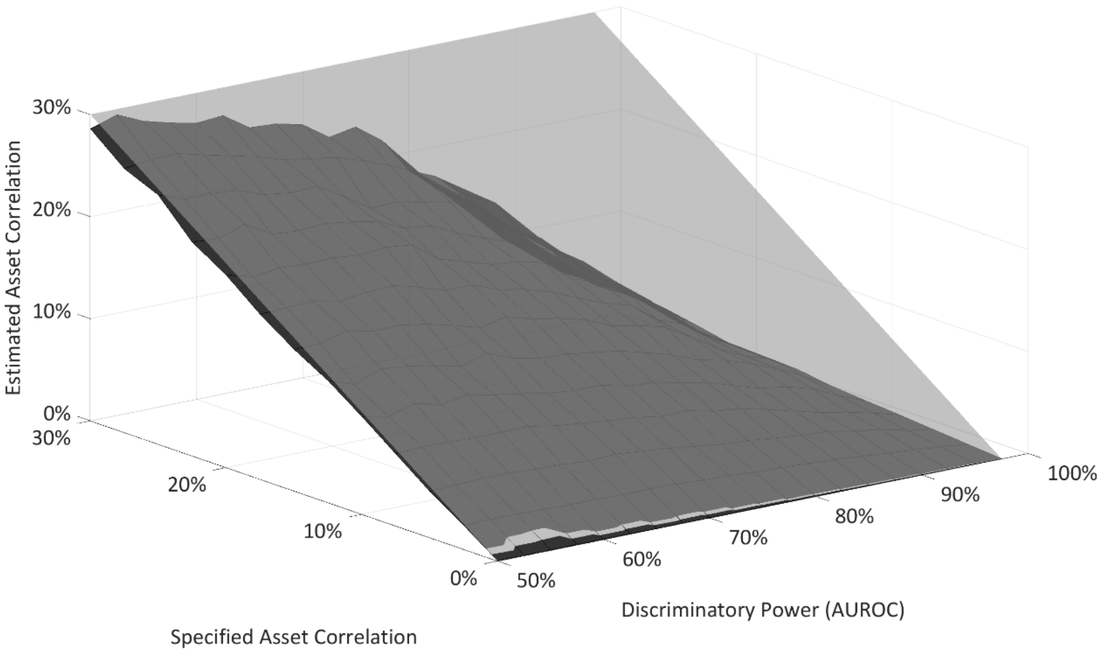

Figure 25: Comparison of theoretical (light grey surface) and average estimated (dark grey surface) asset correlation across 100 random draws of the systematic and idiosyncratic factors, shown as a function of the final (empirical) discriminatory power (measured by the AUROC calculated from the pooled dataset over the entire historical observation period) and predefined asset correlation. The unconditional PD is set to 8.0%. The figure illustrates that asset correlations estimated from time series of default rates (dark grey surface) tend to underestimate the predefined asset correlation (light grey surface). The extent of underestimation of the asset correlation varies with the final (empirical) discriminatory power (AUROC) and the true predefined asset correlation.